

University of California, San Diego



Team: No Plane No Gain

UCSD AIAA Student Chapter
AIAA Design, Build, Fly 2016-2017

Table of Contents

	<u>Page</u>
Section 1: Executive Summary	
1.1 Design Process	5
1.2 Key Mission Requirements	6
1.3 Final Capabilities	6
Section 2: Management Summary	
2.1 Project Management	7
2.2 Milestone Chart	7
Section 3: Conceptual Design	
3.1 Mission Requirements	9
3.2 Score Sensitivity Analysis	10
3.3 Translation to Design Requirements	12
3.4 Solutions, Configurations and Results	12
3.5 Final Conceptual Design	17
Section 4: Preliminary Design	
4.1 Design and Analysis Methodology	18
4.2 Design and Sizing Trades	19
4.3 Mission Modeling and Optimization Analysis	24
4.4 Lift and Drag Analysis	25
4.5 Stability and Control Analysis	27
4.6 Estimated Aircraft Mission Performance	28
Section 5: Detailed Design	
5.1 Final Design Parameters	30
5.2 Structural Characteristics and Capabilities	30
5.3 System Designs, Component Selection and Integration	31
5.4 Weight and Balance	33
5.5 Flight Performance Parameters	34
5.6 Rated Aircraft Cost Documentation	35
5.7 Mission Performance Documentation of Final Design	35
5.8 Drawing Package	37
Section 6	
6.1 Selection Methodology	42
6.2 Investigation and Selection of Major Components and Assembly Methods	42
6.3 Manufacturing Plan	45
Section 7:	
7.1 Objectives and Schedule	45
7.2 Propulsion Testing	45
7.3 Structural Testing	46
7.4 Flight Testing	46
7.5 Flight Testing Checklists	47
Section 8:	
8.1 Component and Subsystem Performance	49
8.2 Complete Aircraft Performance	51
8.3 Future Work	52
References	53

Tables

	<u>Page</u>
Figures	
Figure 1.1: Conceptual Plane Design	5
Figure 2.1: Team Distribution	7
Figure 2.2: Milestone Chart	8
Figure 3.1: Flight Course	9
Figure 3.2: Score Sensitivity Analysis	11
Figure 3.3 Prototype Proof of Concept	17
Figure 4.1: E214 Airfoil	19
Figure 4.2: Airfoil Showing Lack of Thickness for Structural Members	20
Figure 4.3: In1007, Airfoil with Sharp Leading and Trailing Edges	20
Figure 4.4: Lift Coefficient from XFLR5	21
Figure 4.5: Experimental Drag Polar from XFLR5	21
Figure 4.6: Glide Ratio from XFLR5	21
Figure 4.7: Final Wing Dimensioned Top View (inches)	22
Figure 4.8: Model Flight Path	25
Figure 4.9: Coefficient of Lift versus Coefficient of Drag	25
Figure 4.10: Coefficient of Lift versus Angle of Attack	26
Figure 4.11: Glide Ratio versus Angle of Attack	26
Figure 4.12: Drag Contributions from Major Components	27
Figure 4.13: Horizontal and Vertical Tail Dimensions (inches)	27
Figure 4.14: Moment Coefficient vs Alpha, Moment Coefficient vs Lift	28
Figure 5.1: Load Diagram	31
Figure 5.2: Payload Bay and Spine	32
Figure 5.3: Payload Securement	32
Figure 5.4: Wing Attachment and Structure	32
Figure 5.5: Tail Attachment and Structure	33
Figure 5.6: Simulation Flight Paths for Mission 1 and 2	35
Figure 5.7: Simulation Airspeed for Mission 1 and 2	36
Figure 5.8: Simulation G-Loading for Mission 1 and 2	36
Figure 5.9: Dimensioned 3-view	37
Figure 5.10: Structural Arrangement	38
Figure 5.11: Systems Layout	39
Figure 5.12: Payload Accommodation	40
Figure 5.13: Plane Stowed in Tube	41
Figure 6.1: Manufacturing Plan Gantt Chart	45
Figure 7.1: Master Test Schedule	46
Figure 7.2: Propulsion Testing Results, Configuration 2	47
Figure 7.3: Wingtip Test	47
Figure 7.4: Pre-Flight Checklist	48
Figure 7.5: Final Checks	48
Figure 8.1: Mission 1 Propulsion Data	50

Tables

	<u>Page</u>
Tables	
Table 3.1: Figure of Merit Weighting	12
Table 3.2: Aircraft Configuration	13
Table 3.3: Fuselage Configuration	13
Table 3.4: Propulsion Configuration	14
Table 3.5: Wing Shape Figure of Merit	15
Table 3.6: Wingtip Configuration	15
Table 3.7: Wing Thickness Figure of Merit	16
Table 3.8: Landing Gear Configuration	16
Table 3.9: Tail Configuration	16
Table 3.10: Control Scheme Configuration	17
 Table 4.1: Final Wing Dimensions	 22
Table 4.2: Battery Cells	23
Table 4.3: Battery Splitting	23
Table 4.4: Motor Selection	23
Table 4.5: Estimated Mission Scores	29
 Table 5.1: Finalized Design Parameters	 30
Table 5.2: Critical Structural Elements	31
Table 5.3: Weight and Balance	34
Table 5.4: Mission 1 Flight Performance	34
Table 5.5: Mission 2 and 3 Flight Performance	34
Table 5.6: Rated Aircraft Cost	35
Table 5.7: Simulation Mission Performance Parameters	36
 Table 6.1: Manufacturing Figures of Merit	 42
Table 6.2: Fuselage Fabrication Decision Matrix	42
Table 6.3: Wing Fabrication Decision Matrix	43
Table 6.4: Tail Decision Matrix	44
Table 6.5: Payload Bay Decision Matrix	45
 Table 7.1: Propulsion Testing Configurations	 46
Table 7.2: Flight Testing	48
 Table 8.1: Mission 1 Results	 51
Table 8.2: Mission 2 and 3 Results	51

Section 1: Executive Summary

The following report details the design, fabrication, and testing of the University of California, San Diego (UCSD) Design, Build, Fly (DBF) Team's 2017 competition aircraft. The Team designed an airplane and a launch tube for it to fit in. The system will successfully complete three flight missions and one ground mission. The flight missions consist of an unloaded demonstration flight, a loaded speed flight and a loaded range flight. Loaded flight payloads are 3 hockey pucks, totaling 18 ounces. The ground mission consists of drop testing the tube with the loaded plane stowed inside. The Team plans to successfully complete all missions, and optimize the speed and weight of the plane to achieve the highest score.

1.1 Design Process

In order to maximize the flight score, the Team started with a design that would result in a fast, lightweight aircraft to minimize wing area and therefore tube dimensions. By identifying critical metrics and criteria, the Team selected a design from a list of possible conceptual designs. During the preliminary design phase, the Team also compared and chose an appropriate battery, propeller, and motor configuration to best accommodate both the selected design and competition requirements. Initial sizing considerations began using historical data from winning reports published by AIAA. The Team performed lift, drag, and weight analyses as well as trade studies to determine the optimal configuration for the plane. During the detailed design phase, mechanisms for stowing the plane in the tube were designed, and tube configuration and design was finalized.

The Team selected a modular conventional high wing airplane shown in Figure 1.1, consisting of a spine on which the fuselage, wing, tail and motor are mounted. The plane will carry a maximum of 3 hockey pucks for loaded missions. The plane stows in the tube by rotating the wing along a main mounting bolt to become parallel to the fuselage as shown in Figure 1.1.

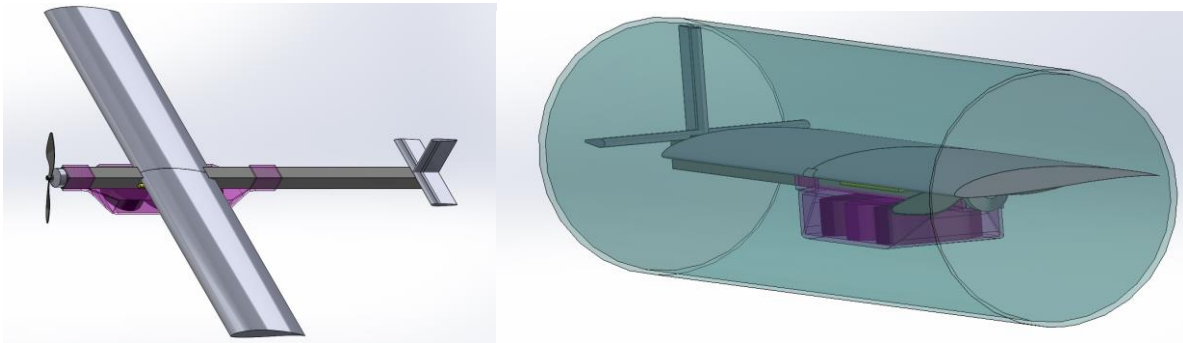


Figure 1.1: Conceptual Plane Design

The modular design allows for rapid iteration of prototypes, and the ability to change individual aspects of the design for flight testing. The stowing mechanism for the wing is simple, and minimizes the cross sectional area of the tube. Carrying 3 hockey pucks at 60mph will provide a high mission score for missions 2 and 3.

1.2 Key Mission Requirements

The DBF competition consists of three flight missions and one ground mission. The flight missions are performed by flying laps around a figure-8 flight course of at least 2000ft in distance traveled per lap. Mission 1 is an unloaded flight; a passing score is awarded if 3 laps are flown within 5 minutes. Mission 2 is a speed flight; the plane will complete 3 laps as fast as possible while carrying 3 hockey pucks. Mission 3 is a range flight; the plane will carry the maximum number of pucks for the maximum number of laps within a 5-minute window. The ground mission is a loaded drop test. The loaded plane is stowed in the tube and dropped 3 times from a height of one foot: once on each end and once on its side (length parallel to the ground). The Team identified 3 important design elements to maximize final score: empty weight, cruise speed, and toughness.

Empty weight is a key factor because its value is included in the Rated Aircraft Cost (RAC), a divisor for the overall score. Also, a lighter aircraft lessens the stress on the tube in the drop tests. The Team elected to use lightweight composites, plastic and foam for main structures on the plane, in order to minimize weight.

Cruise speed is important because the fastest plane in the competition will receive the highest mission 2 score, and will likely achieve the highest overall score for mission 3 as well. To maximize cruise speed the Team focused on propulsion choice, minimizing drag and cross-sectional area. The Team selected to only fly three hockey pucks for mission 3, the same payload as mission 2. This allowed the Team to design a single-role aircraft for five minutes of top speed flight with an 18-ounce payload. The propulsion system, fuselage and payload bay were optimized to meet this goal.

Aircraft toughness is a key factor. The plane is a belly-lander to minimize drag, so the aircraft will contact the ground on every landing and needs to be tough enough to handle the repeated stress. A Kevlar/carbon fiber composite was chosen for main structures for its abrasion and impact resistant properties. The plane will also need to handle the impacts of being dropped inside the tube. Any assemblies that will take impact from the tube or the ground were designed with safely surviving these impacts in mind.

1.3 Final Capabilities

The final mission capabilities of the aircraft from flight data are reported below:

- Capable of hand launch with and without 18-ounce payload
- Completes 1 loaded lap in approximately 50 seconds with payload
- Collapses to be stowed in a tube for ground drop tests
- Capable of 5 minutes of endurance at nominal required cruise speed

The remainder of this report details the design requirements and processes the Team used to arrive at the final design. Final aircraft fabrication, flight tests, and optimizations are ongoing. The Team will use the remaining weeks to finish fabrication of the final aircraft and tune it for competition.

Section 2: Management Summary

2.1 Project Management

The project team is led by two project managers, and divided into five sub-teams with individual leads as shown in Figure 2.1. Sub-teams allow for greater focus on each sub-system; each sub-team has around 5 members. The Project Managers share administrative tasks and supervision of plane design and manufacturing. The Aerodynamics Team utilizes Computational Fluid Dynamics (CFD) programs to size lifting surfaces, analyze drag, and assess stability. The Propulsions Team selects the motor, battery, and propeller using constraints set by the other sub-teams. The Propulsions Team also verifies propulsion performance using a motor test stand. This team must understand the interplay of weight and power, as both are critical for power system design. The Structures Team requires knowledge of material properties, use of Computer Aided Design (CAD), and Finite Element Modeling (FEM) software to design load-bearing components and select materials. The Fabrication Team requires skills with shop tools and manufacture of composite materials to oversee prototype production. The Flight Team requires the ability to operate the aircraft in flight and to perform flight tests to gather data. The Report Team requires technical writing skills; the team will work with the other teams to compose the proposal and report.

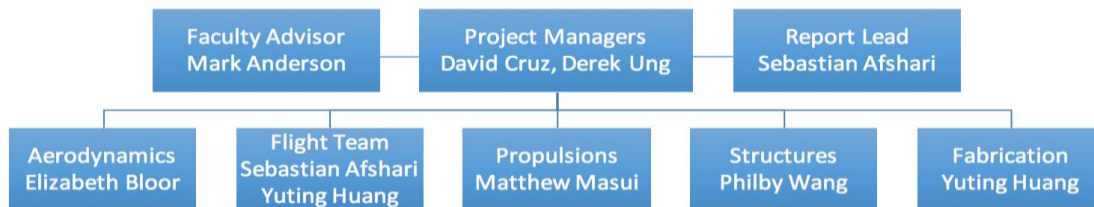


Figure 2.1: Team Distribution

2.2 Milestone Chart

A Gantt chart shown in Figure 2.2 tracks milestones and progress of the design, production, and manufacturing of individual components and the overall plane. Highlighted areas show which component of the project the Team is working on during that specific week, and stars denote milestones. The Gantt chart helps the Team stay updated on which component is being worked on during any specific week, and the overall progress of the project.

University of California San Diego

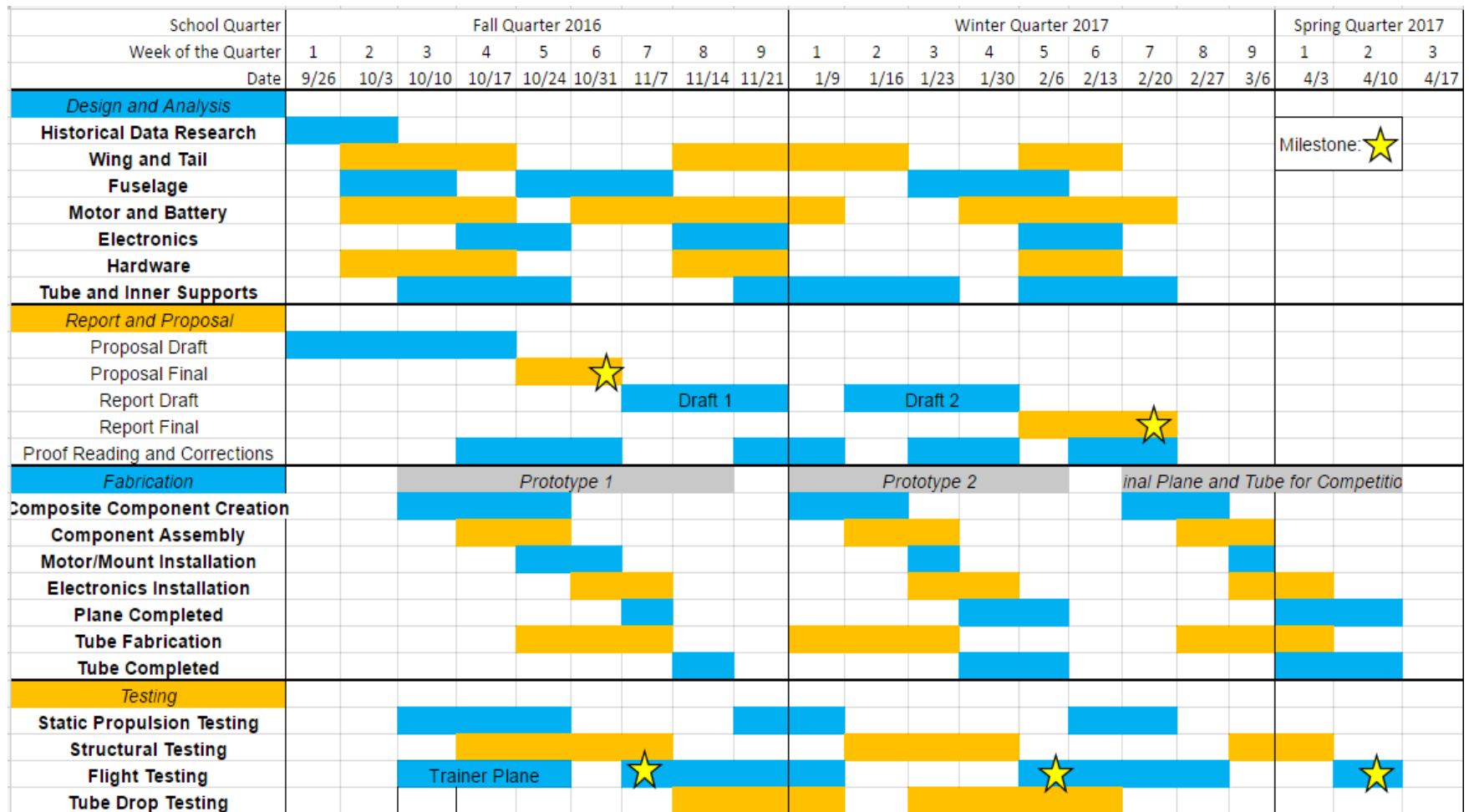


Figure 2.2: Milestone Chart

Section 3: Conceptual Design

3.1 Mission Requirements

3.1.1 General Requirements, Limitations and Concerns

The following are some general requirements for the competition:

- The aircraft must land safely in order to receive a score for each flight.
- The aircraft must be hand launched.
- The aircraft must pass a loaded tip test.
- The aircraft must self-lock and transition into flight configuration.

Flight missions are composed of flying various payload configurations around a specified course depicted in Figure 3.1. The course is figure-8 shaped with 1000 foot straight sides and two 180 degree turns of arbitrary radii. After its first turn, the plane must make one 360 degree turn of an arbitrary radius opposite to the 180 degree turns, creating a figure 8 pattern. Flight mission distance is set in laps around this circuit.

Flight missions must be completed in order (1, ground, 2, 3) and none may be skipped.

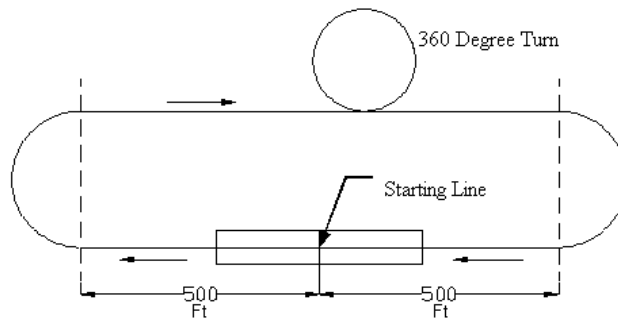


Figure 3.1: Flight Course

3.1.2 Flight Crew

The flight crew is composed of 3 people: the pilot who flies the plane, the ground crew who throws the plane and changes payloads, and the observer who tracks the plane for the pilot and alerts the pilot of any notifications or flag signals.

3.1.3 Mission 1 – Demonstration Flight

For the first mission, the plane completes three laps within a five-minute window without payload. A successful flight gives mission score (M1) of 1.

3.1.4 Mission 2 - Speed Flight

For the second mission, the plane completes three timed laps as fast as possible with a payload of three regulation hockey pucks. The mission's score (M2) consists of a ratio of the fastest time for any Team and the flight time the plane flies. M2 is given by equation 3.1.

$$M2 = 2 * \frac{(Fastest\ Time)}{(Time\ Flown)}$$

Equation 3.1: Mission 2 Score

3.1.5 Mission 3 - Range Flight

The plane completes as many laps as possible within a five-minute flight with any number of hockey pucks that the team chooses. An interim mission score is given by the number of laps flown times the number of hockey pucks carried (Laps*Pucks). The mission 3 score (M3) consists of a ratio of the Team's interim score and the highest score of any team. M3 is given by equation 3.2.

$$M3 = 4 * \frac{Laps * Pucks}{MAX(Laps * Pucks)} + 2$$

Equation 3.2: Mission 3 Score

3.1.6 Ground Mission

The plane must be stowed in the launch tube with maximum payload and then dropped from a height of at least 12 inches. The tube will be dropped 3 times, once flat (tube length parallel to ground) and once on each end. The aircraft must then be removed and transitioned to flight configuration, and the plane and tube must show no damage. Parts of the plane may not be removed or separated for stowing, but must hinge and self-lock into place in flight configuration instead. The plane must pass control and structural tests. The mission gives no score but must be passed to fly mission 2.

3.1.7 RAC

The Rated Aircraft Cost (RAC), given by equation 3.3, is a function of maximum aircraft empty weight (W_{t_p}) and launch tube weight (W_{t_t}), length (L), and circumference (C).

$$RAC = (W_{t_p} + W_{t_t}) * (L + C)$$

Equation 3.3: RAC

3.1.8 Overall Scoring

The overall score is a combination of the mission score (% of 100), report score, and RAC. The mission score is given by equation 3.4 and the overall score is given by equation 3.5.

$$Mission\ Score = M1 + M2 + M3$$

Equation 3.4: Mission Score

$$Score = (Report\ Score) * \frac{(Mission\ Score)}{RAC}$$

Equation 3.5: Overall Score

3.2 Score Sensitivity Analysis

The Team focused on mission 3 performance for the score sensitivity analysis. The Team postulated that carrying three pucks as fast as possible is a winning configuration. This would win mission 2 and achieve a good enough score on mission 3 to win the competition. Trying to fly more pucks in the third mission would result in a heavier flying weight and would require heavier batteries. This would result in a higher RAC. Flying three pucks for both payload missions also simplifies the design, and lessens the load held for the drop tests.

A score sensitivity analysis was conducted by plotting the overall score as a function of maximum pucks carried. This analysis was conducted by assuming that the UCSD plane was the fastest for mission 2, and flies at the same airspeed for missions 2 and 3. Using the rule of thumb that propulsion should

provide 50 Watts per pound of takeoff weight, equation 3.6 was generated for empty weight. Each puck weighs 6 ounces, so equation 3.6 relates adding puck weight to required voltage increase and battery weight increase, which affects the empty weight. N_Pucks is the number of pucks flown. Score estimations are inputted for tube sizing and airframe weight which are assumed to be the same for all teams.

$$Empty\ Weight = \frac{Airframe\ Weight + \sqrt{15 + 7 * N_Pucks}}{7}$$

Equation 3.6: Empty Weight as a Function of Pucks Flown for Mission 3

Figure 3.2 shows the results for two UCSD airspeeds (40 and 50 mph). The blue stars indicate UCSD scores for the number of pucks flown for mission 3 while the red line indicates the best score that a team who maxed out mission 3 could get. Using historical data, it was determined that a team focused on winning only mission 3 could fly 8 pucks for 4 laps. Assuming flight speed is the same for missions 2 and 3, the red line shows this score.

The Team only considers this analysis to be accurate up to a 5 puck payload, where larger wings will be required to account for takeoff speed limitations thus increasing empty weight and decreasing flight speed.

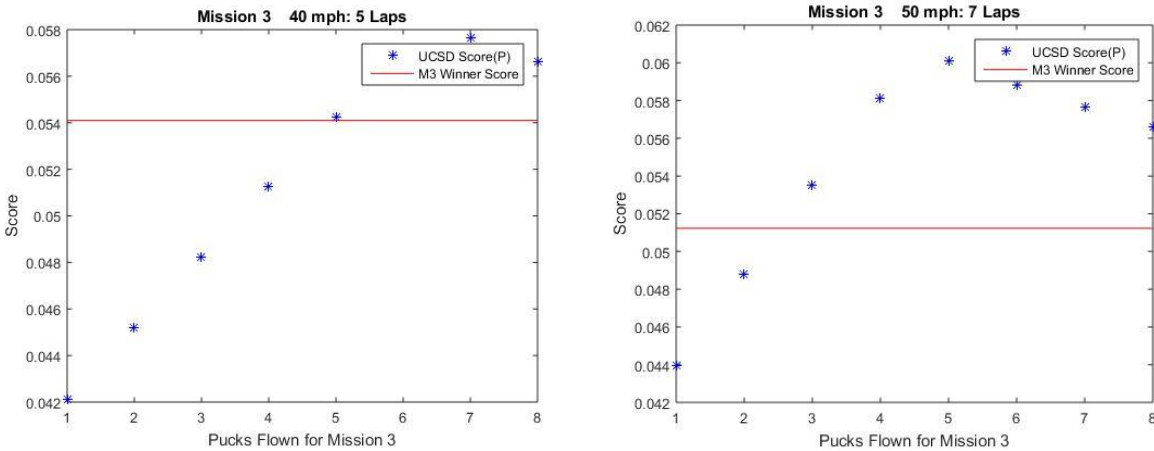


Figure 3.2: Score Sensitivity Analysis

Flying three pucks will not provide the best possible score, but as long as this configuration wins Mission 2 it is possible to beat a team that wins Mission 3 so long as the plane's cruise speed is at least 50 mph. This is because the team with the heavier payload will need to fly heavier batteries, and have a slower airplane. The Team set a 60mph cruise speed as a design specification, which this analysis shows to be a winning configuration. The Team decided not to maximize the score by increasing the number of pucks flown to 5, as this would unnecessarily complicate the plane design.

3.2.1 Propulsion Optimization Analysis

The primary requirements for the selection of the battery and motor for the plane are the flight speed, mission duration, and lap distance. Maximizing flight speed maximizes mission 2 score. The motor must be able to supply the power for this speed. A suitable wattage is calculated based on the weight,

which includes the payload, and energy required for take-off and gravitational effects. With these energy specifications, the aircraft must ascend 100 ft within 4 seconds to allow recovery from gusts and winds. Battery weight is included in the empty weight of the plane, so batteries with the highest energy density are preferable.

3.3 Translation to Design Requirements

Mission 1: Assuming a lap distance of 3000 feet, an aircraft needs to fly at least 40 mph to finish within 3 minutes. The remaining 2 minutes are reserved to account for turning and winds.

Mission 2: The aircraft must be able to carry an 18-ounce payload at a flight speed of at least 60 mph, as determined by the analysis in section 3.2. It also allows for a successful completion of the mission as the 3 laps must be completed within the 5-minute window.

Mission 3: The Team decided that, in order to maximize mission 2 and mission 3 scores, that the aircraft would be designed to carry 3 pucks as fast as possible. This minimizes the aircraft weight for the ground mission and RAC score, while allowing the team to maximize the propulsion system for all missions.

Ground Mission: The aircraft must be able to be stowed within the tube, and supported so that it sustains no damage during handling and drop tests. The tube will have a diameter of less than 8 inches, shortest possible length, and weigh less than two pounds. It will be constructed to sustain no damage when dropped onto a hard surface.

3.4 Solutions, Configurations, and Results

The aircraft was divided into six major design elements: aircraft configuration, fuselage, propulsion system, wings, landing gear, and the tail. Multiple configurations meeting the requirements were accepted for consideration; the options were narrowed down to the optimal selections.

A Figure of Merit (FOM) decision matrix approach was used to gauge the level of optimal performance for each element. A FOM for different variables were weighed on a 100-point scale based upon the variable's importance to the success of the design. More important metrics were given more weight. The different possible choices for each design element were compared against one another by assigning each configuration a score for all metrics. The scores' corresponding meanings are tabulated in Table 3.1.

1	Poor
2	Below Average
3	Average
4	Above Average
5	Excellent

Table 3.1: Figure of Merit Weighting

3.4.1 Aircraft Configuration


			
FOM	Weight	Flying Wing	Conventional
Weight	40	4	5
Collapsed Size	30	1	5
Structural Capability	15	4	4
Manufacturability	10	3	5
Stability	5	3	4
Total	100	295	480

Table 3.2: Aircraft Configuration

The main considerations for the aircraft configuration in Table 3.2 were the weight and collapsed size, because they directly affect overall score. Structural capability was given moderate weight, while manufacturability and stability were weighted low. The Team selected a conventional airplane in order to minimize the cross section of the tube. This airframe can also be constructed modularly, allowing for easy testing of different wing and fuselage combinations, which will minimize the dimensions of the containing tube and maximize score.

3.4.2 Fuselages




				
FOM	Weight	Round	Horizontal Rectangle	Vertical Rectangle
Weight	30	1	3	2
Drag	20	1	2	2
Structural Capability	20	3	2	2
Manufacturability	10	1	3	3
Landing Surface	20	2	3	1
Total	100	160	260	190

Table 3.3: Fuselage Configuration

Weight, drag, and structural capability are the important factors in Table 3.3 when considering the general shape of a fuselage. The absence of landing gear also led to the consideration of the landing surface's durability. With less drag and weight, the aircraft has higher potential speed and less weight also directly improves the overall score. The Team decided on a payload bay with a horizontal rectangular cross section that holds three pucks flat, side by side. This configuration provides the most stable surface for a belly landing, will require less material, is the easiest to manufacture, and will have minimal surface area for friction drag.

3.4.3 Propulsion Systems

The following motor configurations were taken into consideration

- Single Tractor: A single motor mounted at the nose of the plane
- Dual Tractor: Two nacelle-housed motors
- Single Pusher: A single motor mounted behind the wing of the plane.




FOM	Weight	 Single Tractor	 Dual Tractor	 Single Pusher
Weight	35	5	4	5
Aerodynamic Efficiency	20	3	5	3
Stability (CG balancing)	20	5	4	3
Ease of Assembly	25	5	3	3
Total	100	460	395	370

Table 3.4: Propulsion Configuration

As shown in Table 3.4, propulsion systems were scored based on weight, aerodynamic efficiency, stability, and ease of assembly. The single tractor setup is ideal as it has a low weight and is easiest to manufacture. A dual tractor system would have the highest aerodynamic efficiency out of these systems because of clean airflow not obstructed by the fuselage. However, the motors would occupy more space when stowed. The single pusher configuration was problematic as it proposed problems to the CG of the plane and is unsafe for hand-launch.

3.4.4 Wings

The shape of the wing for best performance was determined by weighing ease of fabrication, aerodynamic efficiency, weight and stability. A FOM for the wing shape is included as Table 3.5.




FOM	Weight	Elliptical 	Tapered 	Rectangular 
Ease of Fabrication	25	3	4	5
Aerodynamic Efficiency	30	3	3	2
Weight	25	4	4	3
Stability	20	3	3	5
Total	100	325	350	360

Table 3.5: Wing Shape Figure of Merit

A rectangular wing shape was selected due to its ease of manufacturability and consistent cross-sectional area, which maximizes wing area while fitting inside in the tube. The rectangular wing lost most of its points in efficiency, but still proved to be the best option.






FOM	Weight	Rounded 	Angular 	Hoerner 	None 	Winglet 
Weight	25	4	4	3	5	2
Aerodynamic Efficiency	45	3	2	4	0	4
Ease of Fabrication	30	3	3	3	5	2
Total	100	325	290	345	275	200

Table 3.6: Wingtip Configuration

The Team considered employing rounded, angular or Hoerner wingtips as well as winglets or clean configurations as shown in Table 3.6. Hoerner wingtips were selected as they offered the highest aerodynamic efficiency while being easy to manufacture.

Additional considerations for the wing were Aspect Ratio (AR) and wing thickness. The Team settled on a medium AR (~5) in order to minimize the size of the tube, since the tube's minimum AR is 4. The Team considered wing thicknesses in the medium (10-15%) or high (>15%) ranges, and chose between uniform thickness or wings that would taper in thickness from root to tip. The Team considered ease of fabrication, weight, and structural stability, deciding on a uniform medium thickness as shown in Table 3.7.

FOM	Weight	Medium/Uniform	High/Uniform	Medium/Taper	High/Taper
Ease of Fabrication	55	4	5	3	4
Weight	35	4	2	5	3
Structural Stability	10	4	5	3	4
Total	100	400	395	370	365

Table 3.7: Wing Thickness FOM

3.4.5 Landing Gears

FOM	Weight	Landing Gear	No Landing Gear
Weight	30	2	5
Structural Capability	10	5	0
Manufacturability	20	3	5
Drag	40	3	5
Total	100	290	450

Table 3.8: Landing Gear Configuration

As shown in Table 3.8, the Team selected not to use landing gear because it is the lightest configuration and has no drag. Landing gear was determined to be unnecessary since there is no need for taxiing during takeoff as the aircraft is hand launched and the Team is confident that the structure is sturdy enough for belly-landing

3.4.6 Tails

Multiple tail configurations were considered, as shown in Table 3.9. Considerations included: maximizing surface area for minimum cross section, protection on belly landings, drag, and weight.

FOM	Weight	Ring	Conventional	Box	Double Fin	Triple Fin	Plus
Landing	20	5	2	5	2	2	1
Ease of Fabrication	15	4	5	4	4	4	4
Drag	25	1	5	1	4	3	4
Surface Area	30	3	3	4	4	4	3
Weight	10	2	5	2	4	4	4
Total	100	295	380	325	360	335	310

Table 3.9: Tail Configuration

The Team selected a conventional tail design for its ease of fabrication, low drag, and small surface area compared to the other choices.

3.4.7 Controls

FOM	Weight	Full Control	No Rudder	With Flaps
Weight	30	2	3	2
Complexity	60	2	3	1
Manufacturability	10	2	3	2
Total	100	200	300	140

Table 3.10: Control Scheme Configuration

The Team considered three control schemes: full control (aileron, elevator, rudder), no rudder, and full control with flaps. These choices were compared using weight, complexity and manufacturability. As shown in Table 3.10, the Team selected aileron and elevator control only. Due to lack of taxiing and the ease of belly landing in a crosswind, it was decided that yaw control was not critical.

3.4.8 Tube

The Team considered two tube options, a premade phenolic tube and a custom Kevlar/coremat sandwich tube. The Kevlar tube would be lighter and as strong as the phenolic tube, but since the Team views maximizing launch tube performance as a secondary objective the phenolic tube was selected. The phenolic tube will contain padding near both endcaps to transfer landing loads softly to the fuselage of the plane, so as to not damage foam components. Time permitting, the Team will continue to explore the composite tube as an option before competition.

3.5 Final Conceptual Design

After creating the decision matrices, the Team chose a configuration with the following elements:

- Conventional aircraft configuration without rudder control
- Flat rectangular fuselage with no landing gear
- Single motors/propellers mounted at the nose of the aircraft
- Straight, rectangular, uniform thickness wings with Hoerner wingtips
- 3 hockey puck payload

These designs were selected because they give the Team the best chance of getting the highest possible score and winning the competition. The plane is estimated to weigh only 1.5lbs and is expected to fly fast enough to receive a high score on all missions.



Figure 3.3: Prototype Proof of Concept

Section 4 Preliminary Design

The preliminary design phase allowed the Team to perform basic analyses in each of the main sub-teams: structures, aerodynamics and propulsions. The Team used results of these analyses to select components and materials, added detail to the conceptual design ideas, and finalized a more detailed configuration of the aircraft. The Team used basic real world tests to back up analyses as needed.

4.1 Design and Analysis Methodology

4.1.1 Aerodynamics

The two major aerodynamic parameters considered were airfoil selection and wing sizing. Computation Fluid Dynamic (CFD) analyses were performed to verify the design.

When selecting the airfoil, the Team focused on airfoils that could provide high lift at low Reynolds numbers. The Team also considered using different airfoils at the wing root and wingtip to improve stall characteristics. The Team considered approximately 100 airfoils that provided desired characteristics, narrowed down from thousands of options.

When sizing the wing, parameters such as necessary area, wingspan and wing shape were considered. To determine the wing sizing the Team first calculated the necessary area for the required missions. Then the Team analyzed the benefits of wing configuration and shape. From area and shape, the Team determined the chord and span of the wing.

4.1.2 Propulsion

The propulsion concerns for preliminary design were motor placement, battery endurance, and weight. Details such as pack voltage/capacity, propeller and motor choice will be reserved for detailed design and analysis.

The aircraft batteries must be able to power the plane for 5 minutes, which is the maximum mission time, while being as light as possible. Selection is based off of motor voltage and current requirements necessary to propel the aircraft at the desired specifications. The choice between batteries was ultimately limited to the number of cells and the mAh of the cells, which determines the available voltage and the allowable amount of current draw respectively.

Initial motor selection was sized on wattage per pound of aircraft weight. The initial guideline was set to be 50 watts per pound of flying weight, ensuring sufficient power for flight and maneuvering. This was further refined to ensure that ample thrust was provided to accelerate the plane for hand launch takeoffs.

4.1.3 Structures

Preliminary structural configurations were given to payload containment, as other structural elements could not be finalized until the wing, tail and other components were designed for performance. Due to the modular nature of the plane, the payload bay could be designed independently from other components. The payload bay was designed to contain three hockey pucks, as well as serve as the landing surface for the airplane due to the absence of landing gear.

4.2 Design and Sizing Trades

4.2.1 Aerodynamic Design and Sizing Trades

Proper airfoil selection is key to achieving desired aircraft performance. The thousands of airfoil choices were narrowed down to a hundred airfoils that provide high lift at low Reynolds Numbers (Re). From there the selection was further reduced to 32 choices before the final airfoil of E214 was selected. The E214 Airfoil is shown in Figure 4.1. Factors included in narrowing down and selecting airfoils were performance characteristics at three Re values, calculated using chord length, dynamic viscosity of air, and airspeed in equation 4.1 (reference 1, Anderson): Re at maximum airspeed of 88ft/s (~290 000), Re at takeoff (~105 000), and Re during climb (~250 000). Performance characteristics included stall angle, coefficient of drag, ease of fabrication and structural integrity of the wing. Several high performance choices with high camber or very thin designs were rejected due to difficulty of fabrication and structural weakness.

$$Reynolds\ Number = \frac{(air\ density) * (airspeed) * (chord\ length)}{(dynamic\ viscosity\ of\ air)}$$

Equation 4.1: Reynolds Number Calculation

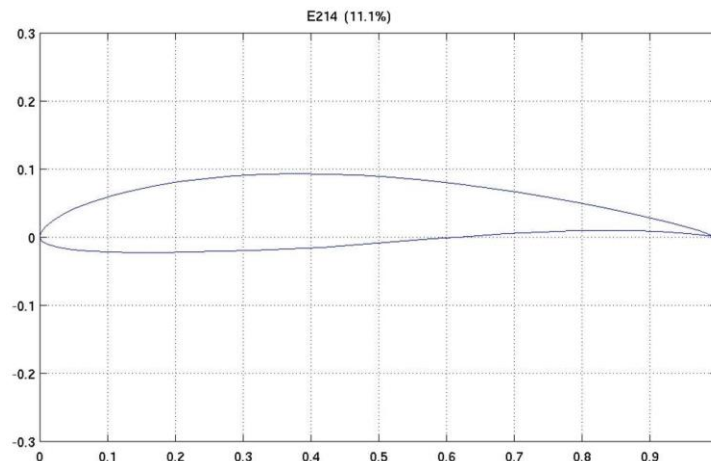


Figure 4.1: E214 Airfoil

Previous years of structural testing have demonstrated that a thickness of at least 10% is needed to provide structural rigidity with light composite and foam construction. Low thickness airfoils do not have high enough inertia or allow enough room for the structural members needed to provide adequate stiffness. The E62 airfoil in Figure 4.2 was rejected for this reason, and is included for reference.

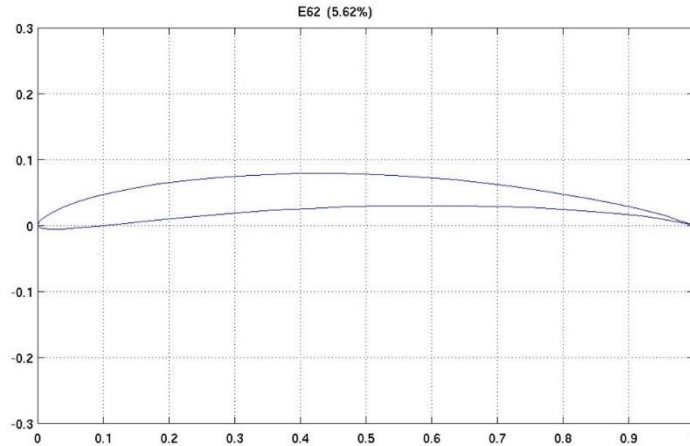


Figure 4.2: Airfoil Showing Lack of Thickness for Structural Members

Additionally, complex airfoil shapes with sharp leading edges and high camber can be difficult to manufacture to design specifications. These airfoils, such as Iln1007 in Figure 4.3, were rejected because imperfections in manufacturing will cause performance characteristics different than those designed.

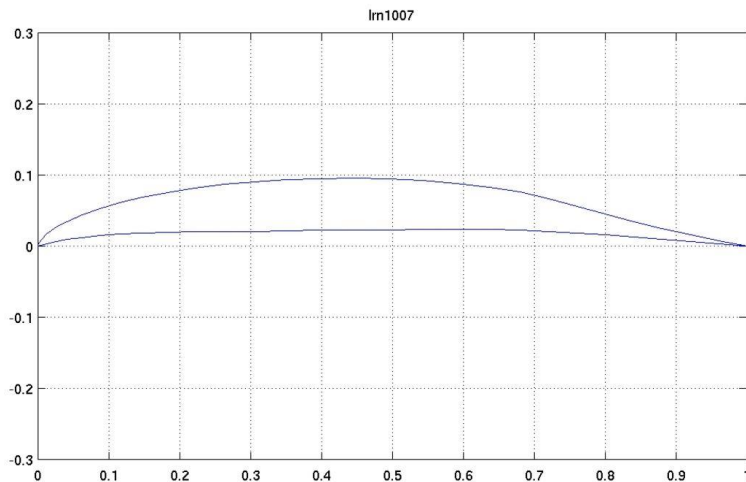


Figure 4.3: Iln1007, Airfoil with Sharp Leading and Trailing Edges

The remaining airfoils were analyzed at the Reynolds numbers listed before (105 000, 250 000, and 290 000). The Team used CFD software XLFR5 to examine the lift, glide ratio, and drag polar to determine optimal airfoils. These analyses for 6 airfoils (E214, E212, E193, S8052, SD9026, SD7043) at Re of 250 000 are included as Figures 4.4-4.6.

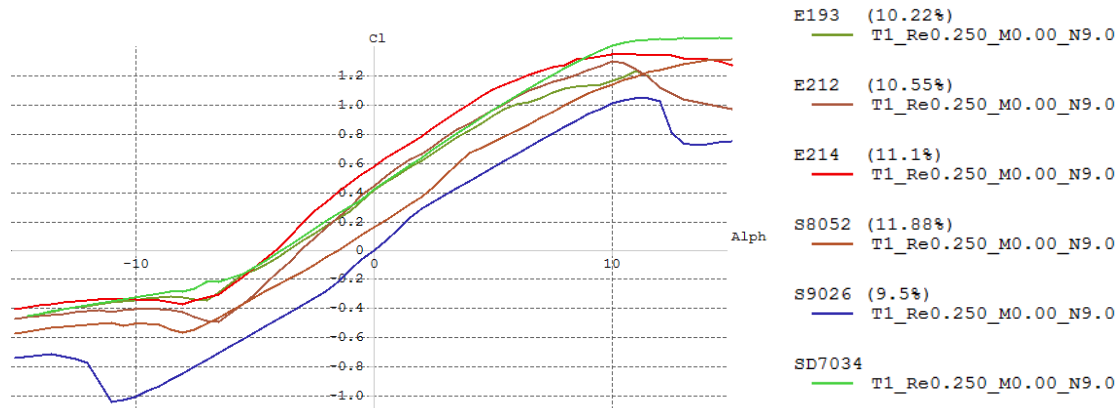


Figure 4.4: Lift Coefficient from XFLR5

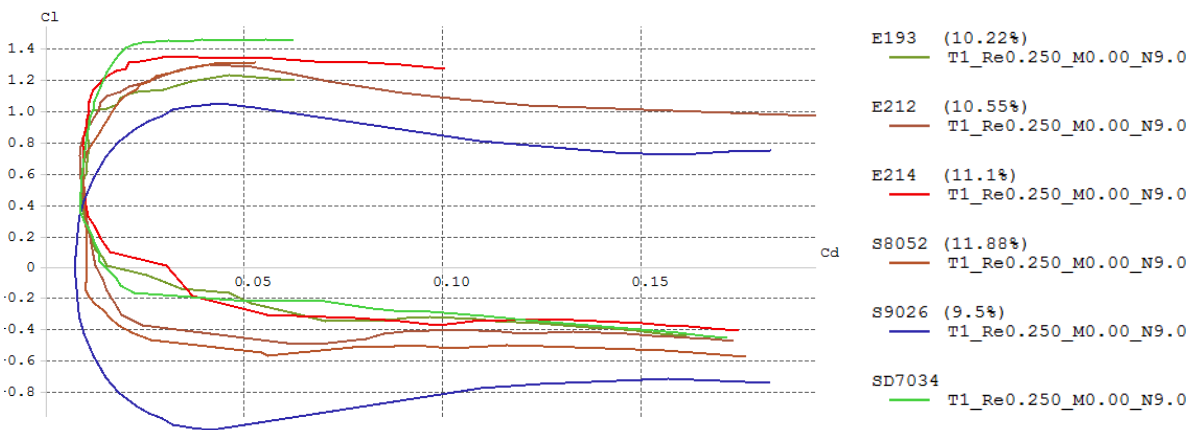


Figure 4.5: Experimental Drag Polar from XFLR5

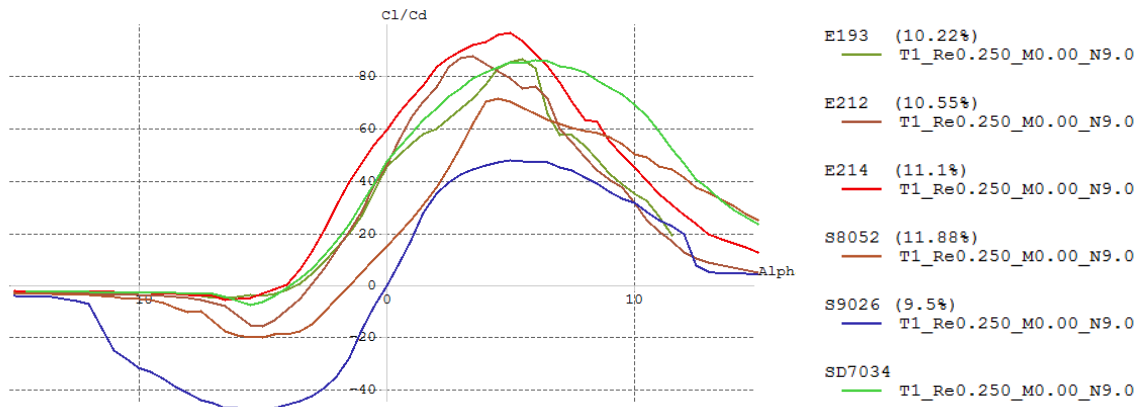


Figure 4.6: Glide Ratio from XFLR5

From the analysis, the Team determined that the E214 airfoil is the best choice. E214 has high camber, sufficient thickness for structural stability (11.1%) while minimizing drag, and a high C_L at the Re for the plane. Finally, examination of the drag polar shows that the Drag Coefficient (C_D) remains low and constant over a large range of C_L which indicates consistent efficiency despite variable flight conditions (wind, downwash, etc.).

The Team sized the wing based off of the predetermined structural weight (32oz) and payload weight (18oz) at takeoff, total weight (W_{calc}) was found to be 40oz (3.125lbs). This weight was inputted in the lift equation, equation 4.2 (reference 1), along with density of air (ρ , 1.199 oz/ft³) which was corrected by a factor of .95 for air density in Tucson, takeoff velocity (V_{TO} , 30mph or 44ft/s), and takeoff C_L (1.15). This information is used to solve for the wing area (A) which was found to be about 1.25 ft.

$$L = W_{calc} oz * 32 \frac{ft}{sec^2} = .5 * \rho \frac{oz}{ft^3} * \left(V \frac{ft}{sec} \right)^2 * A ft^2 * C_L$$

Equation 4.2: Wing Area Calculation from Lift Equation

The Team decided that in order to minimize the cross sectional diameter of the launch tube, the maximum chord (c) could be 6 inches. Using this constraint, the Team solved for a wingspan (s) of 30 inches using equation 4.3 (reference 1). This gives an aspect ratio (AR) of 5 as solved using equation 4.4.

$$A = 1.25 ft^2 = 180 in^2 = span * chord$$

Equation 4.3: Wingspan Calculation

$$Aspect Ratio = \frac{span}{chord}$$

Equation 4.4: Aspect Ratio Calculation

The Ailerons were sized to be 15% of the area of the wing, based off of historical data on remote control airplane design. The ailerons are on the trailing edge close to the wingtips, with a span of 3 inches and a chord of 2 inches.

Final wing dimensions are given in Table 4.1, a dimensioned drawing is provided as Figure 4.7.

Description	Dimension
Wing Span	30 in
Wing Chord	6 in
Wing Area	1.25 ft ²
Aspect Ratio	5
Aileron Span (each)	3 in
Aileron chord	2 in
Wing Airfoil	E214

Table 4.1: Final Wing Dimensions

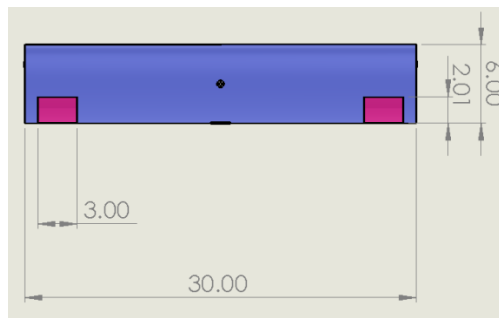


Figure 4.7: Final Wing Dimensioned Top View (inches)

4.2.2 Propulsion Design and Sizing Trades

Conceptual design and sizing trades for the propulsion of the aircraft center around battery cell choice and propulsion motor choice. Due the restriction of battery type to Nickel Metal Hydride (NiMH) or Nickel Cadmium (NiCd) the Team selected to use NiMH which is more energy dense. NiMH cells provide 77.3-78.3 Wh/kg (nominal voltage*capacity) as opposed to 48.5 Wh/kg with NiCd. Energy analysis sets the power requirement to 200W with payload and 130W empty. Battery pack shape is also important, as it effects how it will be stored and potentially impacts aircraft aerodynamics or structures. The Team narrowed the battery cell choices to the three cell types shown in Table 4.2. The Elite 1500 cells yielded an overall lower internal resistance when charging and produced a lower voltage drop when drawing current. These were determined to be the final choice for construction of the flight pack.

Battery Description	Capacity [mAh]	Weight [Ounces]	Size [Inches]	Chemistry
Elite 1500 2/3A	1500	0.81	1.1 x 0.7 x 0.7	NiMH
Elite 2100 4/5A	2100	1.15	1.7 x 0.7 x 0.7	NiMH
Tenergy 2200 SC	2200	2.00	0.9 x 0.9 x 1.7	NiCd

Table 4.2: Battery Cells

Based on the two available cell types, the battery packs can be split as shown in Table 4.3 to generate enough power for a 5-minute flight.

Capacity [mAh]	Cell Count	Weight [Pounds]	Voltage [Volts]	Max Continuous Draw [Amps]
1500	12	0.61	14.4	15
2100	10	.72	15.0	21

Table 4.3: Battery Splitting

The motor selections are chosen based upon their compatibility with the battery packs as well as other factors. Important factors for the plane's motor were both the kV and Wattage ratings, as well as its weight. Higher kV outrunner motors tend to be smaller, while smaller kV tend to be larger, thus affecting the weight contribution of the motor. Another important factor is choosing the correct propeller. However, due to the propeller having a much larger range of options, the Team decided to first choose the motor, then fit an appropriate recommended propeller in the preliminary stages. Motor options that were considered are shown in Table 4.4, these preliminary choices will be analyzed and a final selection will be detailed in Section 5 of this report.

Motor	kV	Max Watts (W)	Weight (oz)
Scorpion SII 2215	900	237	2.42
E-Flite Park 480	910	250	3.07
T-Motor MT 2216	1100	260	2.65
T-Motor AT 2216	1250	260	2.40

Table 4.4: Motor Selection

4.2.3 Structural Design and Sizing Trades

The plane is based around a carbon fiber spine, which has a hollow square cross-section of 1-inch side length. Carbon fiber was selected for this feature due to its small deformation for large applied loads. This property, coupled with the large cross sectional moment of inertia, gives the spine adequate stiffness for flight.

The payload bay is constructed entirely out of composite materials, mostly carbon fiber with a Kevlar landing surface for a bottom layer. The use of composites minimizes the weight of the assembly, and the Kevlar provides resistance to abrasive belly-landings. The payload bay was sized to hold 3 hockey pucks in a row flat along the spine, with fairings fore and aft of the main bay. Though the fairings add material and complexity, they provide for a low-drag configuration.

The Team decided to construct other structural elements out of composites, foam, and plastic, to minimize weight and provide greatest strength. The motor mount is 3D printed in PLA, to allow for rapid motor swaps, and to easily manufacture the complex shape. The wing is constructed entirely out of foam, with a carbon fiber strip wrapping the length of the wing along the one-quarter chord location, acting as a spar. The tail surfaces are constructed from foam with uni-directional carbon fiber tow for stiffeners. All elements are bolted, clamped, or glued to the main spine.

The launch tube will be made of phenolic cardboard tubing, with plastic end caps. The fuselage of the plane will be supported by foam padding, and no other components will contact the tube.

4.3 Mission Modeling and Optimization Analysis

In order to predict performance during flight, the Team created a mission model in MATLAB. With this model, the Team can input relevant vehicle information (thrust, weight, lift, drag, max speed, etc.) and receive an output file detailing flight path, performance parameters, and time information. Overall results are displayed in section 4.6 and 5.7, and are used to decide on optimal configurations. Figure 4.8 shows the modeled flight path that was divided into the following elements:

- Launch (red): The aircraft starts with a 20mph velocity at hand launch
- Liftoff (blue): The aircraft achieves minimum flight speed of 30mph and begins a climb to 100ft.
- Straightaway 1 (gold): after achieving altitude the aircraft flies level until flag 1 (500ft from launch)
- 180 degree turn 1 (green): after passing flag 1 the aircraft initiates a 180 degree right turn
- Straightaway 2 (purple): After completing the 180 degree turn, the aircraft flies level for 500 feet
- 360 degree turn (black): The aircraft completes a 360 degree left turn.
- Straightaway 3 (Grey): After completing the 360 degree turn the aircraft flies level to flag 2 (500 ft)
- 180 degree turn 2 (Brown): After passing Flag 2 the aircraft initiates a 180 degree turn.
- Straightaway 4 (Pink): after completing the 180 degree turn the aircraft flies level for 500 feet returning to its starting point and completing a lap.

All subsequent laps start from Straightaway 1 Section of flight, typically only the first lap is modeled.

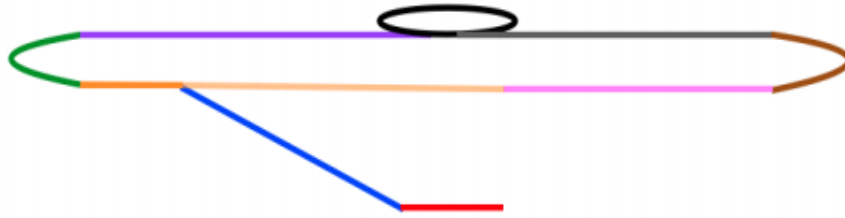


Figure 4.8 Model Flight Path

4.3.1 Mission Model Uncertainties

The mission model is only a rough estimation of flight performance, and carries many inherent uncertainties. Not all components (such as the motor) will perform ideally during actual flight, and there may be discrepancies in weight, lift, and drag parameters of the final aircraft due to variations in manufacturing. This creates uncertainties in the parameters inputted into the model, such as thrust, weight, and cruise speed. Additionally, wind is neglected in the model, and so the presence of wind at competition will change expected performance. Finally, the mission model assumes maximum cruise speed for straight flight, and 2.5g or 1.5g turns, but the inputs of the pilot will differ from the ideal path analyzed in the mission model. All of these factors contribute to uncertainties in the mission model, which represents ideal conditions and is expected to vary slightly from actual flights.

4.4 Lift and Drag Analysis

4.4.1 Lift Analysis

The Team examined the coefficient of lift, coefficient of drag and coefficient of moment (C_m) using XLFR5. The analysis was performed at three Reynolds numbers (takeoff, climb and cruise) as well as for the empty plane (mission 1) and the fully weighted plane (mission 2). Plots of C_L vs C_D , C_m vs Angle of Attack (Alpha), C_L vs Alpha, and C_L/C_D vs Alpha are included in Figures 4.9-4.11.

The C_L vs Alpha, only focuses on the linear portion of the curve, and can be assumed accurate up to an alpha of about 12 degrees.

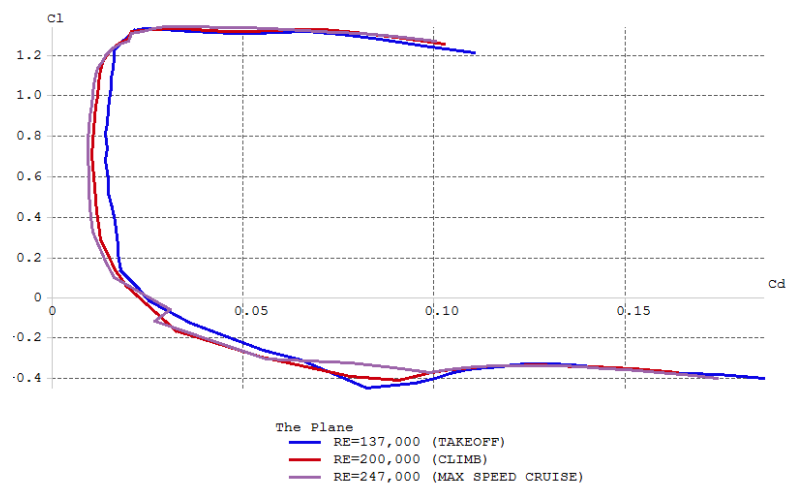


Figure 4.9 Coefficient of Lift versus Coefficient of Drag

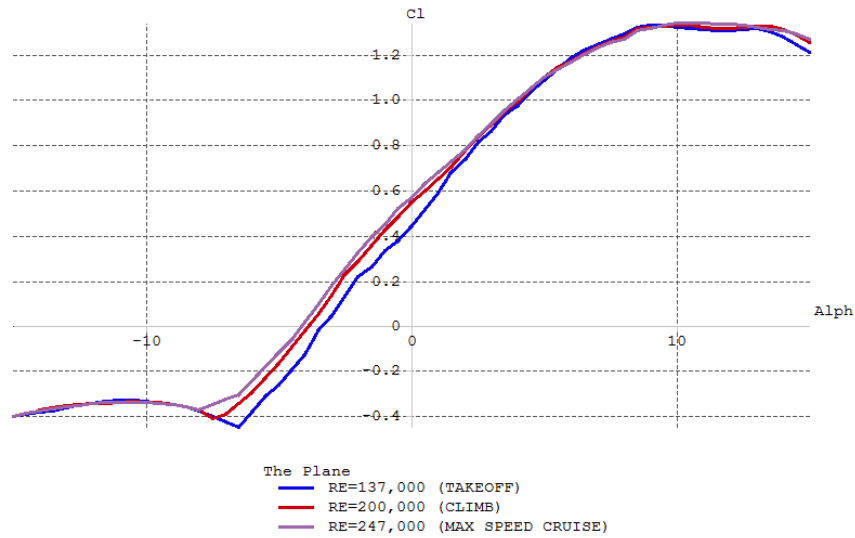


Figure 4.10 Coefficient of Lift versus Angle of Attack

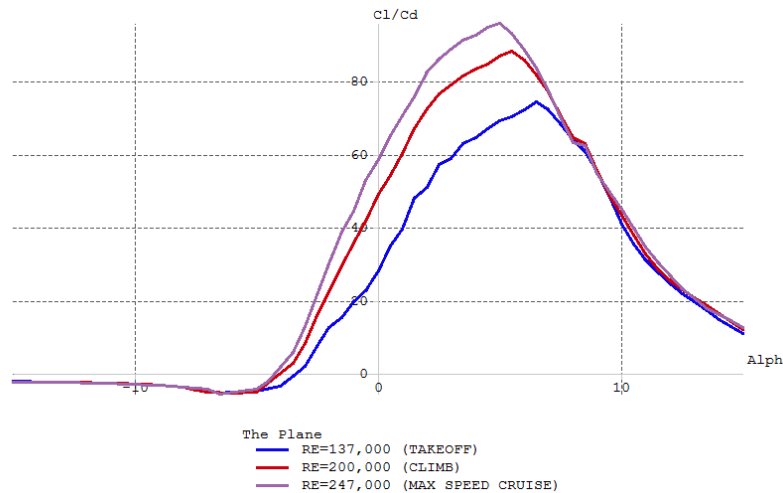


Figure 4.11 Glide Ratio versus Angle of Attack

4.4.2 Drag Analysis

Drag on an aircraft comes from two main sources: parasitic drag, due to the shape of the aircraft and the “wet” surface area (i.e., the amount of surface area exposed to airflow), and induced drag, a by-product of lift. When analyzing the drag characteristics of the aircraft, the Team focused on the parasitic drag because it is a function of aircraft structural and aerodynamic design. Induced drag, on the other hand, is a function of wing planform shape, aspect ratio, and flight conditions. The Team estimated the zero-lift parasitic drag coefficient (C_{D0}) to be .055 using StarCCM+ aerodynamic analysis and the equivalent skin friction method.

The drag distribution, due to different components, is shown in Figure 4.12. As expected, the wing and fuselage have the largest effect on overall drag, contributing over 75%. This is due to the large planform area and large wetted area, respectively.

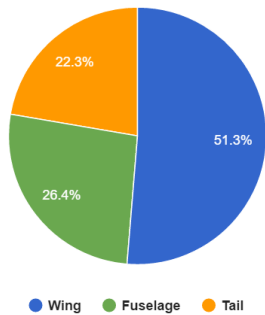


Figure 4.12 Drag Contributions from Major Components

4.5 Stability and Control Analysis

4.5.1 Horizontal Tail

The Team sized the horizontal tail using the tail volume coefficient equation, equation 4.5 (reference 2, Stanford), which solves for the horizontal tail volume coefficient (V_h) using the distance between wing center of pressure (CoP) and horizontal tail CoP (I_h), wing area (A_w), horizontal tail area (A_h) and mean aerodynamic chord of wing (\bar{C}). The equation is solved for tail area by setting $V_h=1$, yielding an area of 39 in^2 . In order to minimize the extents of the plane in the folded configuration, the tail span was set to 6.5 inches and the chord to 6 inches.

$$V_h = \frac{I_h * A_h}{A_w * \bar{C}}$$

Equation 4.5: Tail Sizing

The Team sized the elevator to be around 30% of the horizontal tail chord, based off of historical remote control airplane design. The elevator spans the entire tail with a chord of 2 inches. Horizontal tail dimensions are shown in Figure 4.13.

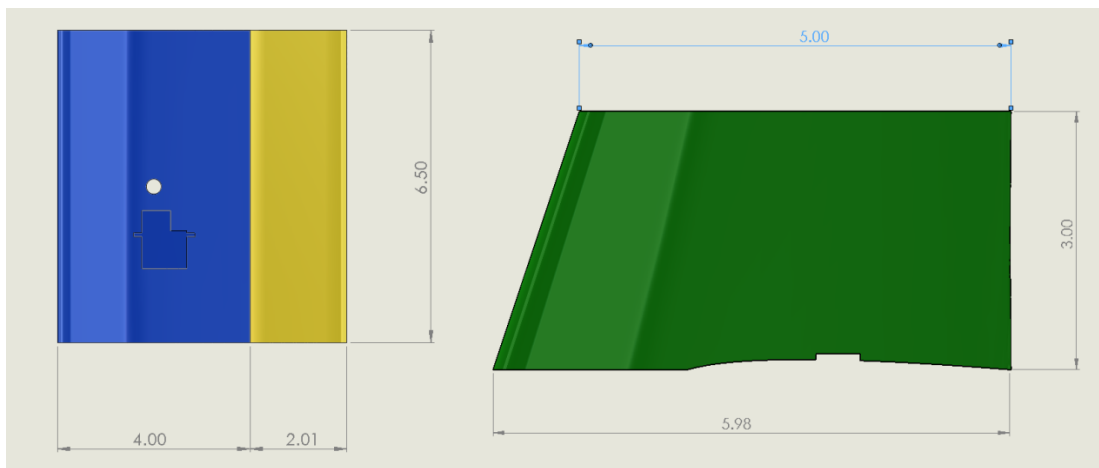


Figure 4.13: Horizontal and Vertical Tail Dimensions (inches)

4.5.2 Vertical Tail

The Vertical tail was sized using the same equation as the horizontal tail, with the vertical tail area, CoP location, and volume exchanged for the horizontal tail values. The equation was solved by

setting vertical tail volume coefficient $V_v=0.06$, yielding a tail area of 17.5 in^2 . In order to minimize cross-sectional extents of the plane the height of the vertical tail was set to 3 inches, with a root chord of 6 inches and a tip chord of 5 inches. Vertical Tail Dimensions are shown in Figure 4.13.

4.5.3 Stability Analysis and Static Margin

To be longitudinally balanced, the aircraft requires the total pitching moment coefficient at zero lift to be positive and for the center of gravity to be ahead of the neutral point. To be statically stable, the slope of the total pitching moment coefficient vs alpha should also be negative when the total pitching moment coefficient is zero. Longitudinal stability analysis was done using XFLR5 given the structural dimensions of the aircraft. The static margin (S.M.) was calculated using equation 4.6 (reference 2) for both unloaded and loaded missions according to C.G. location with respect to the x-axis (X_{cg}), neutral point location (N.P.) and mean aerodynamic chord MAC.

$$S.M. = \frac{N.P. - X_{cg}}{MAC}$$

Equation 4.6: Static Margin

Figure 4.14 shows that the plane satisfies requirements for longitudinal stability. Since the analysis estimated the neutral point at 2.385 in from the leading edge and the center of gravity at 1.5 in, the static margin is positive 0.1475. As the static margin is positive, the aircraft will return to the previous angle of attack if its stability is disturbed. Care will be taken to ensure that the center of gravity is not placed behind the expected value for any flight configuration, as this would result in an unstable configuration.

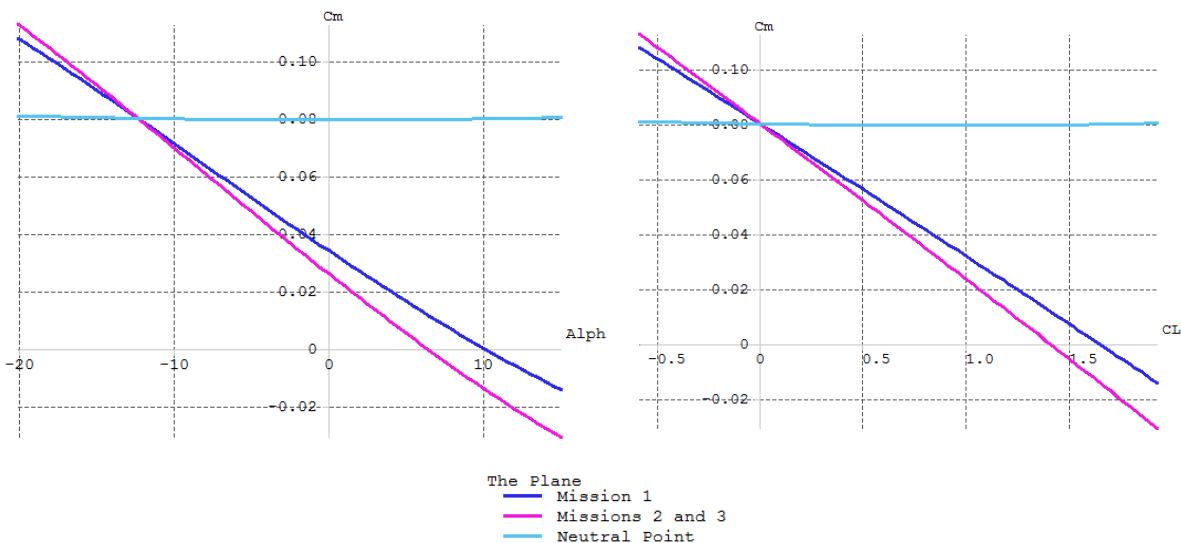


Figure 4.14: Moment Coefficient vs Alpha, Moment Coefficient vs Lift.

4.6 Estimated Aircraft Mission Performance

With the preliminary design of the aircraft completed, the Team was able to use mission modeling analysis to estimate mission performance. The estimated mission performance is reported in Table 4.5.

The scores for Mission 2 and 3 cannot be accurately determined but the Team predicts a competitive performance. Time requirements for Missions 2 and 3 are from historical performance standards for winning teams. Performance estimates show that the aircraft is not fast enough to achieve what the Team predicts as a required winning time. Due to the uncertainties in the mission model, the Team determined that the times were close enough to the requirement to go ahead with the design. If needed, after the prototype has demonstrated that it can reliably complete all 3 missions, efforts will be made to improve the time.

Mission 1		Mission 2		Mission 3 (3 pucks)	
Lap Time (s)	41	Lap Time (s)	55	Lap Time (s)	55
Time Required (s)	100	Time Required (s)	43	Time Required (s)	43
Mission 1 Score	1	Mission 2 Score	?	Mission 3 Score	?

Table 4.5: Estimated Mission Scores

Section 5 Detailed Design

In the final stages of design, the Team finalized component decisions and worked on optimizing the aircraft for each mission. This analysis included flight performance predictions for each mission.

5.1 Final Design Parameters

The finalized design parameters, including electrical, structural and mechanical components are outlined in Table 5.1.

Overall Dimensions		Fuselage (incl. bay)	
Length	40 in	Length	40 in
Width	30 in	Width	3.25 in
Height (prop folded)	5 in	Height	2 in
Wing		Vertical Tail	
Span	30 in	Root Chord	6 in
Ave. Chord	6 in	Tip Chord	5 in
Area	180 in ²	Height	3 in
Aspect Ratio	5	Area	31.5 in ²
Horizontal Tail		Motor/Battery	
Chord Length	6 in	Motor	Scorpion SII 2215 900kv
Span	6.5 in	ESC	ICE2 HV45
Area	39 in ²	Battery Cell	1.2V 1500mAh NIMH
Controls		Number of Cells	12 in series
Servo	hs-5152mg	Volts	14.4 V
Stall Torque (oz.in)	42	Max Amps	18 A
Speed (sec/60deg)	.17	Max Power	260 W

Table 5.1: Finalized Design Parameters

5.2 Structural Characteristics and Capabilities

When designing the aircraft structures, the Team started by considering where loads would be applied and distributed through the structures. The Team first created sketches detailing the places where external loads would be applied, included as Figure 5.1.

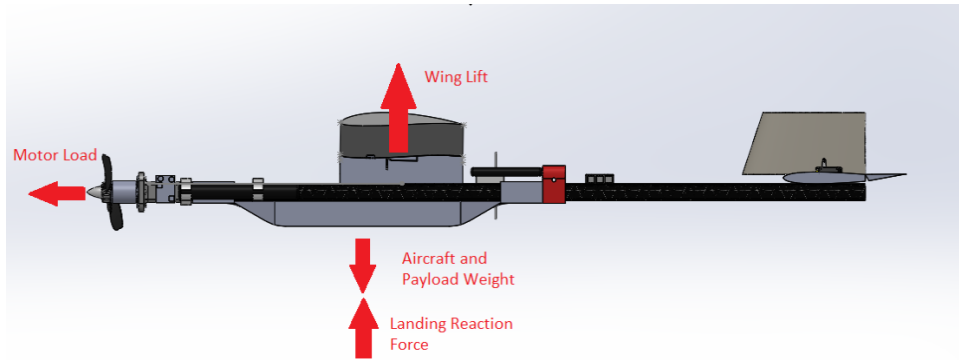


Figure 5.1: Load Diagram

By studying the external loads and the load paths, the Team was able to identify critical load locations on the aircraft. This allowed for design to avoid structural failure at an expected load location. The structural elements, associated loads, and design solutions are detailed in Table 5.2.

Structural Element	Applied Load	Description of Design
Payload Bay	Landing impact	Several layers of carbon fiber to absorb landing impact. Outer Kevlar layer for abrasion resistant skid.
Spine	Point loads from all element connections	Hollow carbon beam of large cross-sectional area to prevent bending or failure.
Wing and Tail Connections	Aerodynamic Loads	Nylon bolts connect the aerodynamic surfaces to the spine, transferring lift forces to spine.
Wing Structural Spars	Tension and Compression from Aerodynamic Loads	Uni-directional carbon fiber wrapped around the quarter chord location supports aerodynamic loads.
Motor Mounts	Torque and Tension from Motors	A plastic 3D printed motor mount fits around the spine and is pinned in place.
Launch Tube	Drop Impact	The plane is supported internally so that the only load it sees is its own weight, transferred to the tube along the spine.

Table 5.2 Critical Structural Elements

5.3 System Designs, Component Selection and Integration

5.3.1 Fuselage Structural Design

The fuselage structure houses the payloads and provide an aerodynamically beneficial shape for load transfer. The Team designed the fuselage modularly, with a carbon fiber spine on which a payload bay is mounted shown in Figure 5.2. The spine is an “off the shelf” hollow carbon fiber tube, with a 1 square inch carbon fiber cross section.

The payload bay is mounted below the tube, under the center of gravity location. The main structure is constructed 0/90 Kevlar weave for abrasion and impact protection on landings.



Figure 5.2: Payload Bay and Spine

5.3.2 Payload Securement

The payload bay is sized to exactly contain 3 hockey pucks, with little room for shifting, as shown in Figure 5.3. The bay will be loaded separate from the spine, covered, and then bolted to the plane. This guarantees the containment of the payload, and that the center of gravity does not shift during flight. Payload bay location ensures that unloaded and loaded flight configurations have the same center of gravity.



Figure 5.3: Payload Securement

5.3.3 Wing Structure

The wing is constructed out of foam with uni-directional carbon fiber laid span-wise along the quarter-chord location as a spar. The wing shape is cut out of foam using a hot wire cutting system. The spar is then wrapped around the wing and left to cure in a vacuum bag. The final wing structure is shown in Figure 5.4.

5.3.4 Wing Attachment System

The wing is secured to the spine by a main mounting bolt that goes through the spar location, as can be seen in Figure 5.4. This bolt transfers the aerodynamic loads to the spine of the plane. In order to pin the wing in place, a thin sheet of polycarbonate is mounted on the underside of the wing near the trailing edge. An inclined plane forces the sheet to flex upwards until it falls into a gap, latching only when the wing is perpendicular to the spine, the device locks the wing into the flight configuration. Flexing the sheet up allows the wing to rotate to become parallel to the fuselage for stowing.

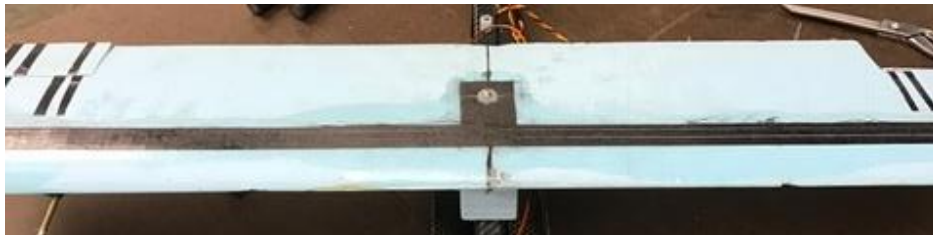


Figure 5.4: Wing Attachment and Structure

5.3.5 Tail Structure and Attachment

The tail is constructed in the same manner as the wing, however the spar is constructed from uni-directional carbon fiber tow. The tail is bolted to the rear of the spine; this and the structure are depicted in Figure 5.5.

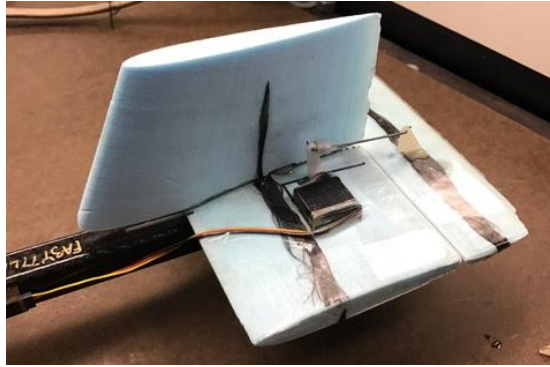


Figure 5.5: Tail Attachment and Structure

5.3.6 Electronic Control System

The Team selected the Spektrum DX6i transmitter with the AR636 6 channel receiver. The receiver has a built in 3 axis control system, and the Team will be able to adjust gains to improve flight stability and performance. The control system will be tuned by the pilot observationally during flight tests. The Team chose Hitec HS-5152MG servos because of their slim (10 mm) profile, which allows for easy integration in the wings with minimal effects on aerodynamics.

5.3.8 Propulsion System

The final propulsion configuration is the Scorpion S11 2215, 900 kv motor, powered by a 12 cell 14.4v 1500mAh NiMH battery pack. This setup provides 260W peak power and a pitch speed of 72 feet/sec when coupled with an 11in x 8in folding propeller.

5.3.9 Tube

The launch tube is store-bought and constructed out of resin impregnated cardboard. The plane is supported internally on each end by mounting the spine directly to the endcaps. The rest of the plane is cushioned with soft foam. The stowed plane can be seen in Figure 5.13 of the Drawing Package in section 5.

5.4 Weight and Balance

Component weights, locations from the firewall (x distance), and locations above the thrust line (z distance) are included in Table 5.3, along with the resultant weight and CG locations for all configurations. Distances in the y direction are not considered because the plane is symmetric about the centerline (x-z plane).

	Weight (oz)	X distance from motor mount (in)	Z distance (thrust line is Z=0) (in)
Fuselage	1	4.7	-1.6
Motor	3	-1.4	0
Batteries	3.6	4.88, 19.12 (avg. 11.5)	0
Receiver	0.4	21.9	0
Wing	4	9.6	0.7
Spine/mounts	11.2	12	0
Tail	5.8	31.6	0.75
Payload	18	11.2	-1
M1 (empty) total	29	14	.19
M2 Total	47	12.94	-.27
M3 Total	47	12.94	-.27

Table 5.3: Weight and Balance

5.5 Flight Performance Parameters

Using the aerodynamic data from CFD analyses, the Team identified relevant flight performance parameters for various angles of attack representing level flight, cruise and takeoff. These values are listed in Table 5.4 for Mission 1 and Table 5.5 for Missions 2 and 3.

Angle of Attack (deg)	C_{Lmax}	C_{D0}	Turn Rate (deg/sec)	Wing Loading (lb/in ²)	Takeoff Weight (lb)
0	0.42900	0.09800	39.53	0.01111	2
1	0.50600	0.01500	48.12	0.01111	2
8	0.99200	0.05675	100.26	0.01111	2

Table 5.4: Mission 1 Flight Performance

Angle of Attack (deg)	C_{Lmax}	C_D	Turn Rate (deg/sec)	Wing Loading (lbm/in ²)	Takeoff Weight (lb)
0	0.42900	0.09800	7.3	0.02056	3.7
1	0.50600	0.01500	19.8	0.02056	3.7
8	0.99200	0.05675	54.3	0.02056	3.7

Table 5.5: Mission 2 and 3 Flight Performance

5.6 Rated Aircraft Cost Documentation

The Rated Aircraft Cost (RAC) has a high impact on overall score. The Team focused on minimizing weight and tube diameter in order to lower the RAC. The final RAC value is documented in Table 5.6, computed using Equation 3.3.

RAC Parameter	Value
Plane Weight	2 lb
Tube Weight	2.5 lb
Tube Diameter	7.5 in
Tube Length	40 in
Total RAC	213.75

Table 5.6: Rated Aircraft Cost

5.7 Mission Performance Documentation of Final Design

Using aircraft parameters and mission analysis code, the Team was able to calculate estimated performance for each of the missions. This analysis allowed the Team to identify critical stages of flight and identify corresponding deficiencies. In particular, the Team considered: aircraft loading, airspeed, turn rate, bank angle, climb angle, and altitude. Flight path is plotted for missions 1 and 2 in Figures 5.6. Airspeed for one lap is shown by Figure 5.7 and g-loading is shown in Figure 5.8, the markers represent the start of the specified event. From these figures it was determined that at no point in the missions does the aircraft stall, or exceed the maximum acceleration of 2.5g, during turning and level flight. Additional, parameters are included in Table 5.7.

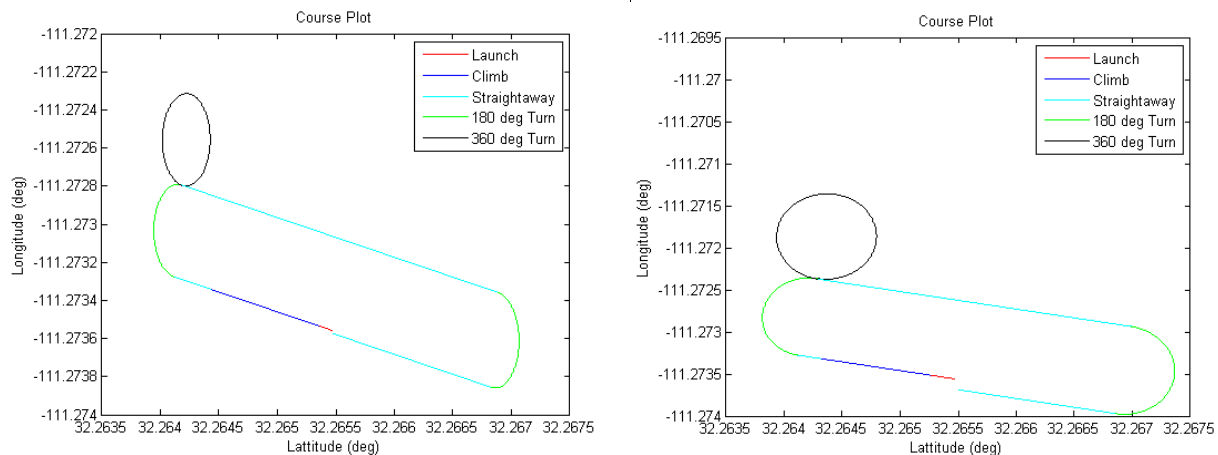


Figure 5.6: Simulation Flight Paths for Mission 1 and 2

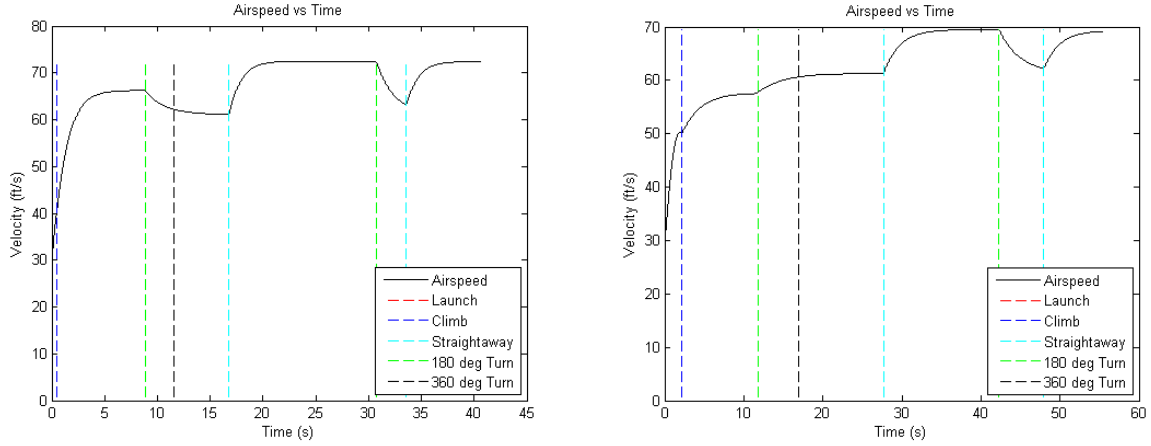


Figure 5.7: Simulation Airspeed for Mission 1 and 2

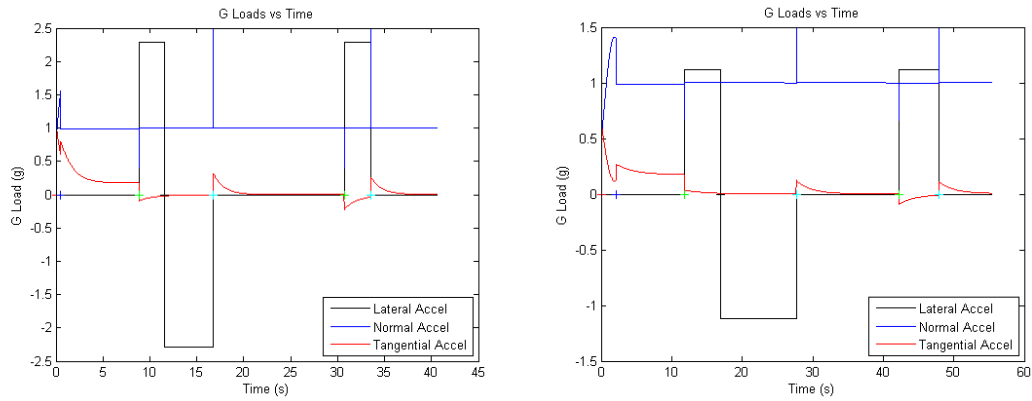


Figure 5.8: Simulation G-Loading for Mission 1 and 2

Mission	Max Normal Load (g)	Cruise Speed (mph)	Turn Rate (deg/sec)	Bank Angle (deg)	Climb Angle (deg)	Lap Time (sec)
M1	2.5	49.38	67.80	66.8	15	40.63
M2	1.5	47.16	35.72	48.2	12.3	55.35

Table 5.7: Simulation Mission Performance Parameters

5.8 Drawing Package

Figure 5.9: Dimensioned 3-View

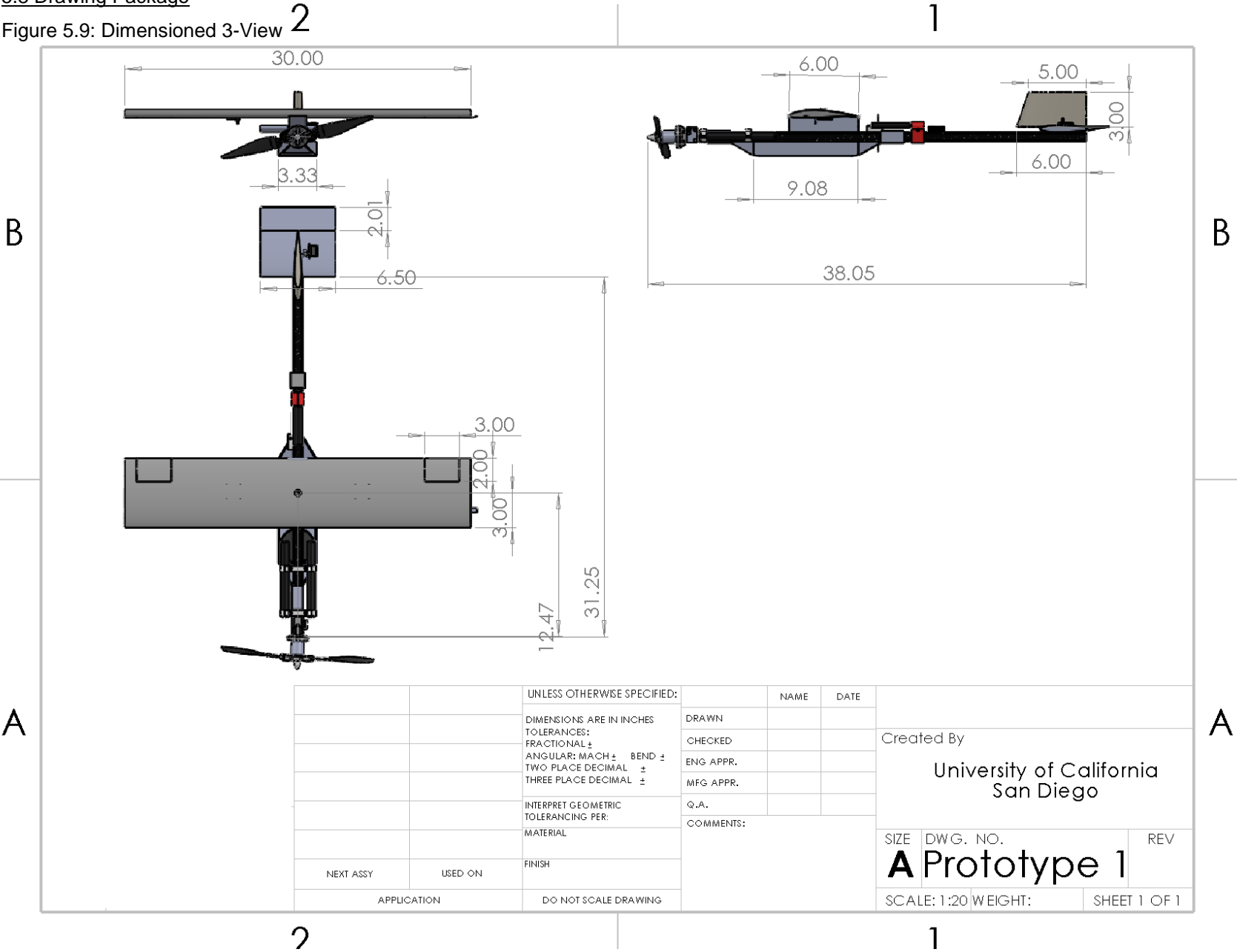


Figure 5.10 Structural Arrangement

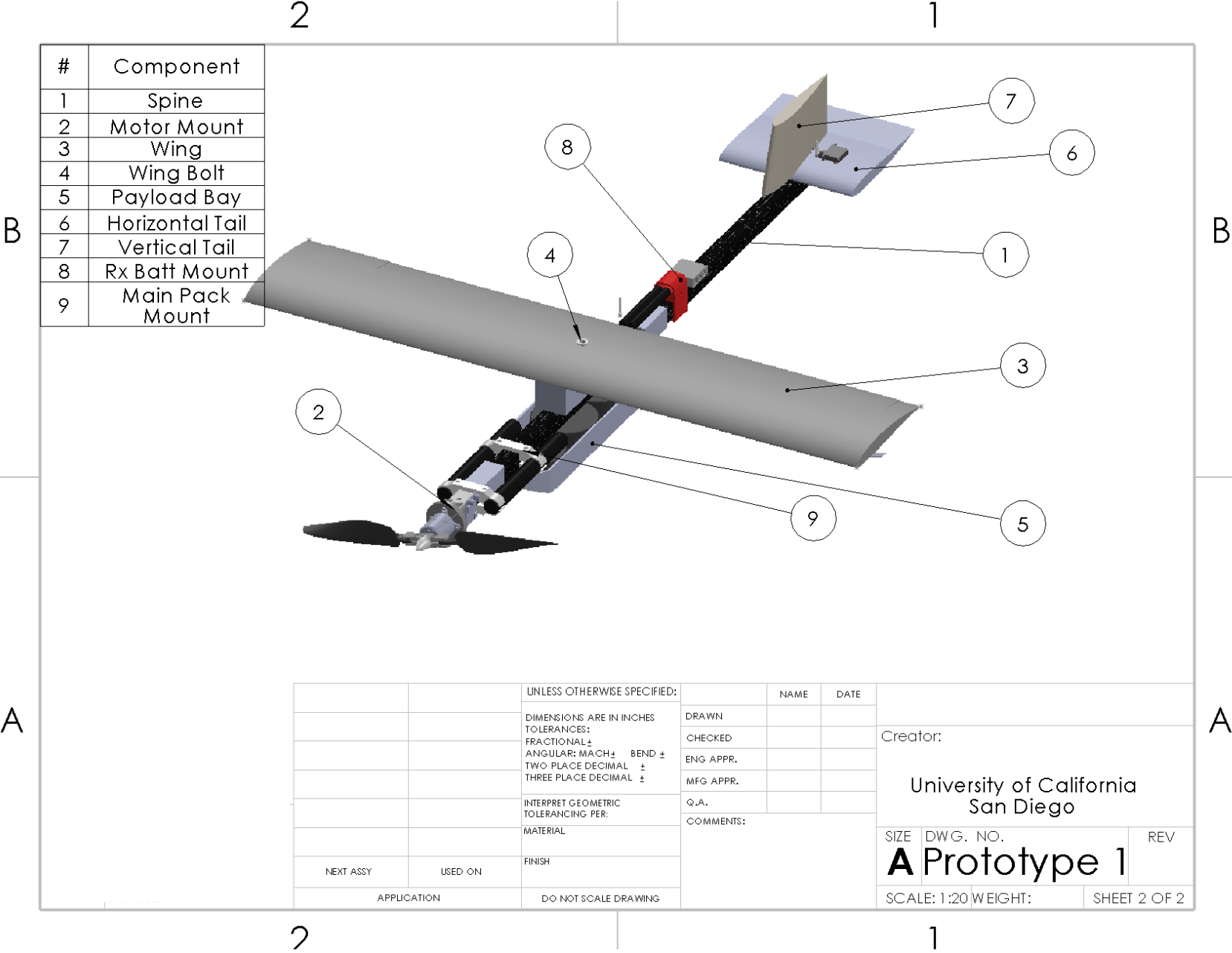


Figure 5.11 Systems Layout

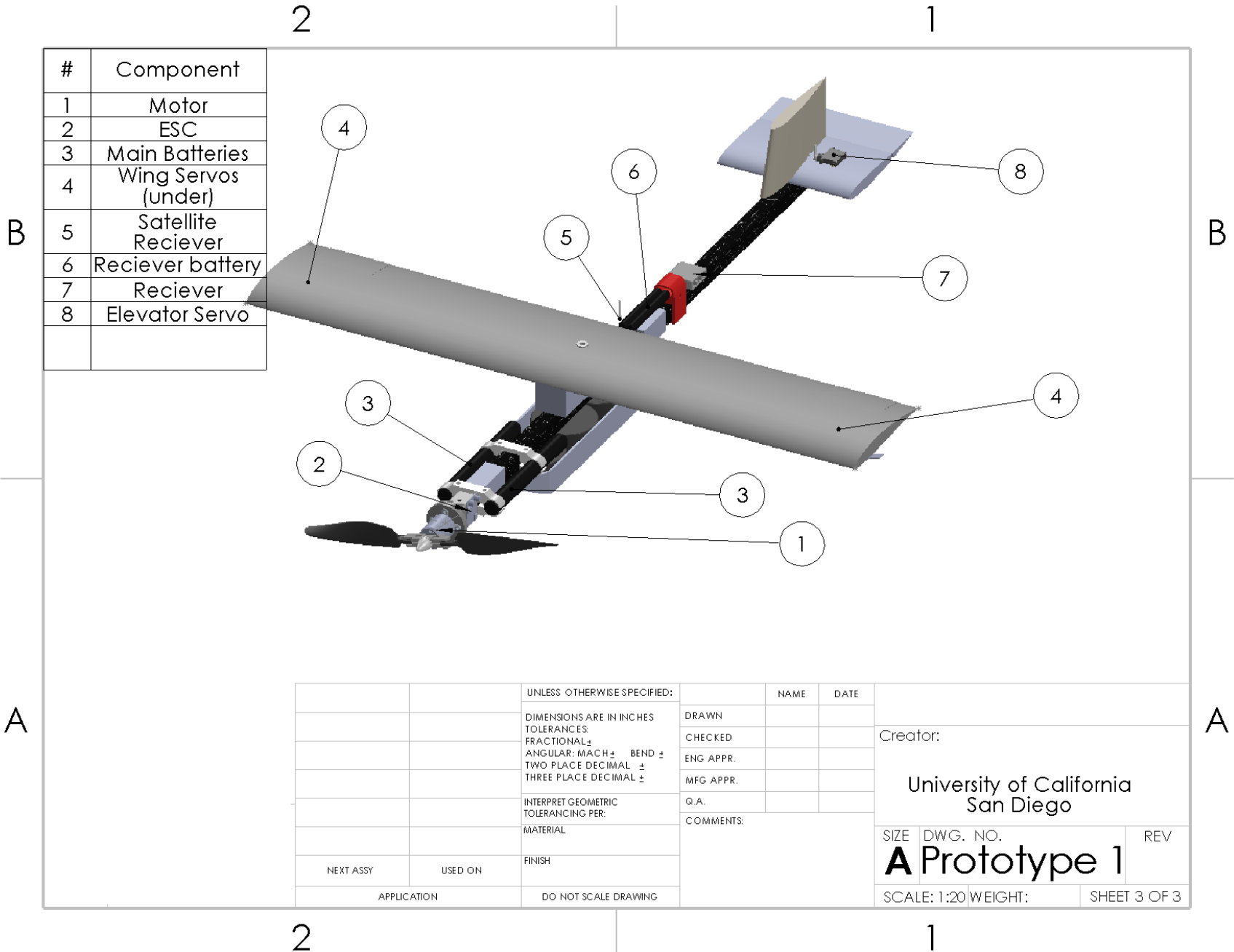


Figure 5.12 Payload Accommodation

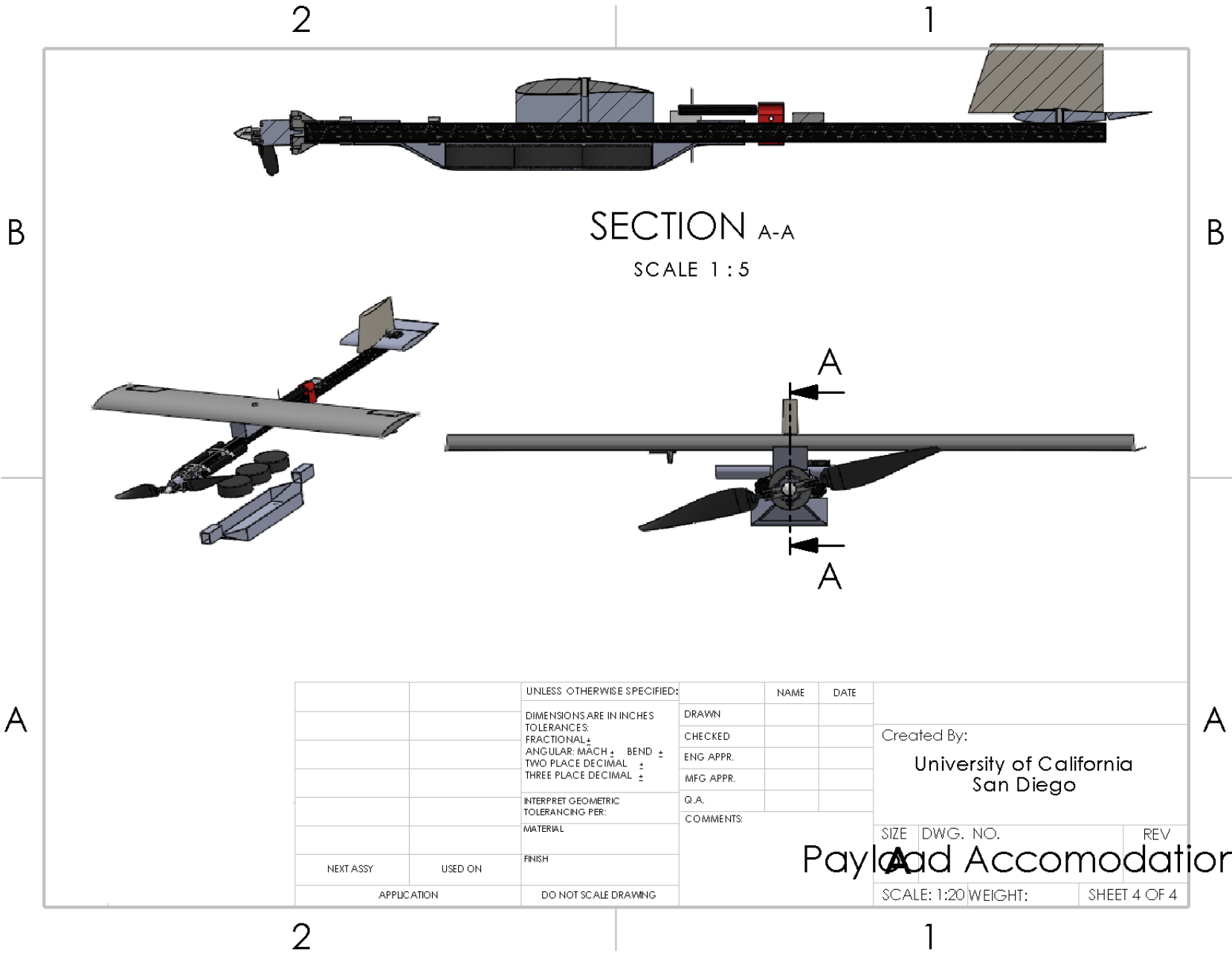
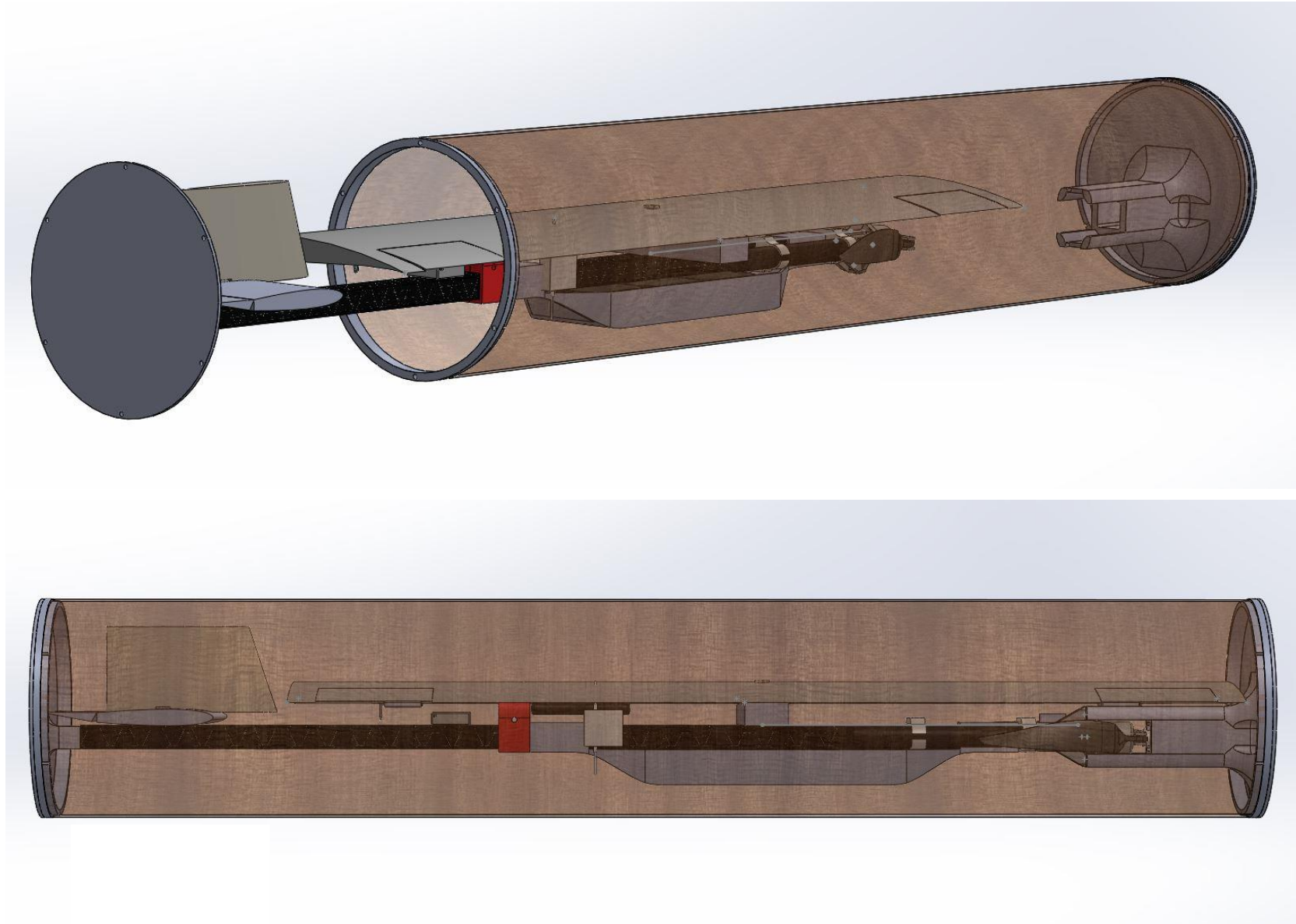


Figure 5.13: Plane Stowed in Tube



Section 6

6.1 Selection Methodology

The Team researched and compared several manufacturing methods and materials for the major components of the aircraft. The Team then selected based on pros and cons with the missions in mind. Five different Figures of Merit were considered, as shown in Table 6.1.

Metric	0	5	10	15	20	25	30	35
Weight							30	
Ease of Fabrication						25		
Ease of Repair		5						
Cost		5						
Strength								35

Table 6.1: Manufacturing Figures of Merit

Strength is required to absorb impact on the drop test, and take flight loads. The decision to omit landing gear and belly land also adds to the strength requirement. Weight was ranked high due to its direct impact on the RAC. The tube-storing requirement also pushed the Team to heavily consider ease of manufacture because designs and mechanisms needed to be iterated quickly.

6.2 Investigation and Selection of Major Components and Assembly Methods

6.2.1 Fuselage

Balsa truss, lost-foam core, and carbon fiber square tube were different methods considered for the construction of the fuselage. These configurations are compared in Table 6.2.

- Balsa Truss: A frame is constructed of balsa wood, then covered in a skin of Mylar.
- Lost-Foam Core: A block of foam is cut in the desired fuselage shape, then wrapped in carbon fiber and given time to cure. The foam is then melted out using acetone, leaving the carbon fiber fuselage shell.
- Carbon Fiber Square Tube: a premade carbon fiber square tube for a primary load bearing spine.

FOM	Weight	Balsa Truss	Lost-Foam Core	Carbon Fiber Square Tube
Weight	30	5	4	5
Ease of Fabrication	25	3	4	5
Ease of Repair	5	3	4	3
Cost	5	5	4	3
Strength	35	3	4	5
Total	100	370	400	480

Table 6.2: Fuselage Fabrication Decision Matrix

The Team ultimately selected the carbon fiber square tube. This design simplifies the manufacturing process as it was bought “off the shelf” and provides low weight and high stiffness and strength. The square tube allows a modular design concept, where all the critical components can be bolted on and removed easily, allowing rapid prototyping of modules. It also provides a flexible adjustment of CG for better balancing.

6.2.2 Wings

The Team considered the following three methods for wing construction:

- Wood Ribs: Airfoil sections are cut out of balsa using a LaserCamm, then connected using thin balsa spars and stringers. The wing is then covered in a Mylar skin.
- Foam Core Composite: A foam wing is cut out using a hot wire CNC, using airfoil shape guidelines at each end. The foam wing is given a carbon fiber spar, and can be covered in a fiber for finish.
- Hollow Composite with Spar: Similar to the foam core technique, but a fiber spar is included at the quarter chord of the wing to add support, and then the foam core is removed with acetone.

FOM	Weight	Wood Ribs	Hollow Composite	Foam Core Composite
Weight	30	5	5	4
Ease of Fabrication	25	3	4	5
Ease of Repair	5	3	4	4
Cost	5	3	3	3
Strength	35	3	4	5
Total	100	360	425	455

Table 6.3: Wing Fabrication Decision Matrix

Foam core is the easiest to manufacture with access to a CNC foam cutter and has great strength and impact resistance, at a slight cost of an increase in weight. The wings are made with foam core, reinforced with carbon fiber. This composites design is chosen considering the strength, weight, and the drop test.

6.2.3 Tail

Wood ribs and foam core were the considered for the construction of the tail. These are the same methods as described for the wing in section 6.2.2.

FOM	Weight	Wood Ribs	Foam Core
Weight	30	5	4
Ease of Fabrication	25	3	5
Ease of Repair	5	3	4
Cost	5	3	3
Strength	35	3	5
Total	100	360	455

Table 6.4: Tail Decision Matrix

The Foam Core was chosen for the same reason as for the wings: its strength, toughness, and ease of manufacture.

6.2.4 Payload Bay

Wood ribs and lost-foam core were the two methods considered for the construction of the payload bay.

- Wood ribs: Airfoil sections are cut out of balsa using the LaserCamm then connected using thin balsa spars and stringers. The entirety is then covered in a Mylar skin.
- Lost-Foam Core: The method is like the foam core technique, but the foam core is removed after the fiber/epoxy are set.

FOM	Weight	Wood ribs	Lost- Foam Core
Weight	30	5	4
Ease of Fabrication	25	3	4
Ease of Repair	5	3	4
Cost	5	3	4
Strength	35	3	4
Total	100	360	400

Table 6.5: Payload Bay Decision Matrix

Ultimately the lost-foam core method was chosen since it is easy to manufacture. The strength is also better than wood ribs. The payload bay is made of carbon fiber and Kevlar, with uni-directional carbon fiber tow reinforcement. The Kevlar is for impact absorption and abrasion resistance for landings.

6.2.5 Motor and Electronics Mounts

All of the mounts for electrical components (including the motor) are constructed out of 3D printed PLA plastic. 3D printing these components allows them to be modeled to fit the complex shapes of the electronics, and be clamped or pinned to the spine.

6.3 Manufacturing Plan

The Team's manufacturing plan, shown in Figure 6.1, allowed the Team to follow a strict schedule of prototype construction. Extra time was allotted in the beginning of the first quarter to allow the new leaders and team members to become adjusted and learn their various respective responsibilities. After the first iteration, the Team was able to speed up the process with a more streamlined work flow, as the work was similar to that which was done before.

Week of the Quarter	2	3	4	5	6	7	8	9		1	2	3	4	5	6	7	8	9			1	2
Payload Bay																						
Wing																						
Tail																						
Assemble																						
Tube																						

Figure 6.1: Manufacturing Plan Gantt Chart

Section 7

7.1 Objectives and Schedules

The Team created and executed a comprehensive testing plan to gather data used to optimize the design of the aircraft. The master test schedule for all subsystems is shown in Figure 7.1, where P# denotes prototype number and F denotes final system. The structures test consists of a wingtip test with max payload; lifting the plane by its wingtips simulates 2.5g loading and verifies structural stability. Additional structural checks will be performed as necessary. The flight tests verify controllability and gather flight data. The mission tests verify that the aircraft can complete the required missions, including the ground missions. Destructive testing involves testing surviving components of the prototype to failure to determine ultimate strength and failure modes.

Week of Quarter	Q2	1	2	3	4	5	6	7	8	9	Q3	1	2
Structural Verification		P1				P2						F	
Flight Testing													
Mission Testing													
Destructive Testing													

Figure 7.1: Master Test Schedule

7.2 Propulsion Testing

Thrust tests were conducted using a motor test stand (RC Benchmark Dynamometer). The flight propulsion system was tested to measure thrust, motor RPM, voltage, and current with respect to ramping the ESC signal. Two configurations were tested as shown in Table 7.1. Figure 7.2 shows the results of configuration 2 testing.

Test Configuration	Motor	Propeller	ESC	Battery	Cell Size
1	SII 2215 900 Kv	11x8F	Castle Thunderbird	Elite 1500mAh NiMH	10
2	SII 2215 900 Kv	11x8F	Castle Thunderbird	Elite 1500mAh NiMH	12

Table 7.1: Propulsion Testing Configurations

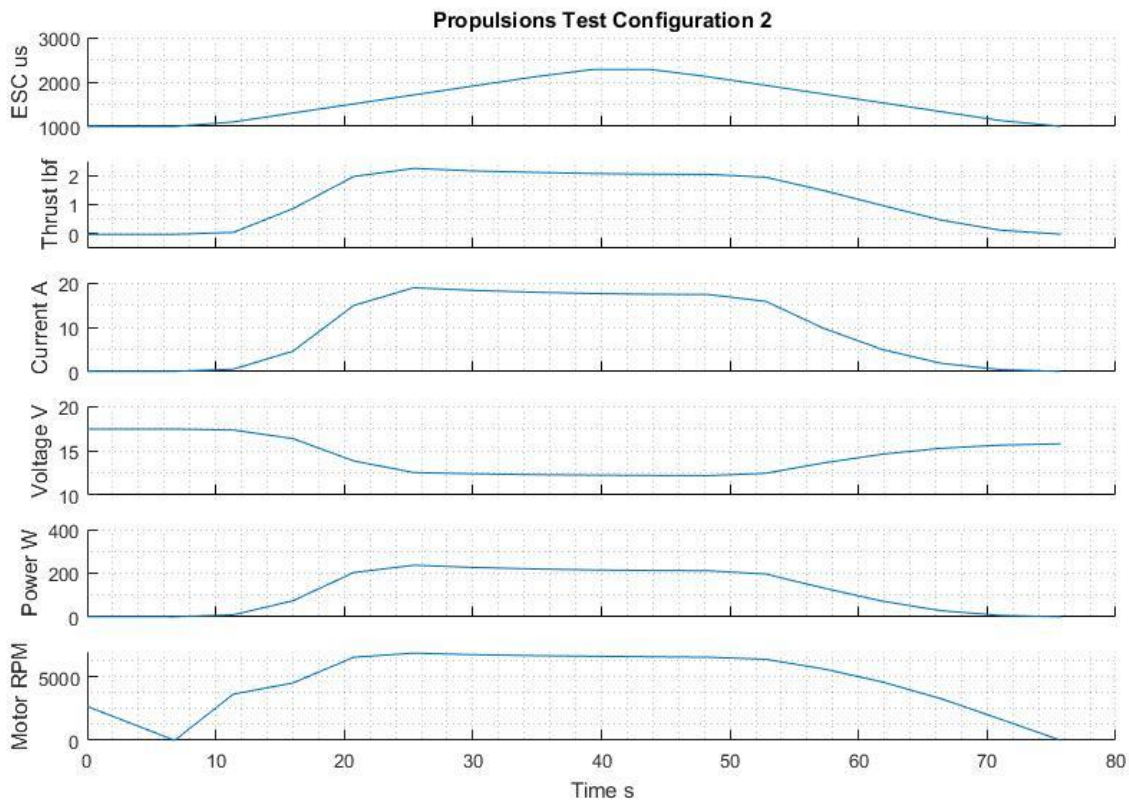


Figure 7.2: Propulsion Testing Results, Configuration 2

Testing has shown that the second configuration provides two pounds of thrust at max throttle, which provides a thrust to weight ratio that is deemed to be sufficient for flight.

7.3 Structural Testing

To verify the structural integrity of the aircraft the Team performed a number of tests on structural elements, namely the wings and fuselages. To test the stresses and structural integrity of the wings, a wingtip test was performed with maximum payload, as shown in Figure 7.3. Additionally, once parts have fulfilled their use for flight tests they will be tested to failure. If parts fail during flight tests the failure mode and flight conditions are recorded.

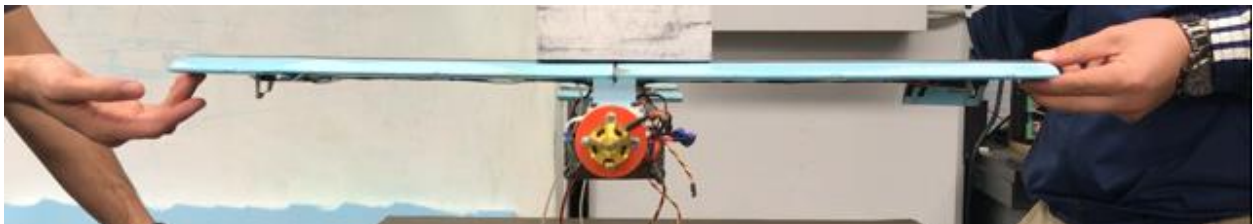


Figure 7.3: Wingtip Test

7.4 Flight Testing

The Team understands the importance of flight tests that do not require full mission performance from the outset. To find and correct instabilities and other unforeseen problems, the test plan in Table 7.2

details the gradual increase in demand on the aircraft. This sequence is followed for every prototype, and restarted whenever a component is changed.

Flight	Payload
Maiden Flight, Tuning	None
Tuning (Repeat as Necessary)	None
Mission 1 Test	None
Mission 2 Test	18 oz
Mission 3 Test	18 oz

Table 7.2: Flight Testing

7.5 Flight Testing Checklists

Checks are performed five minutes prior to flight, and these checks are shown in Figure 7.4.

Pre-Flight Checklist			
Propulsion		Payload	
Right Propeller?	<input type="checkbox"/>	Weight Verified?	<input type="checkbox"/>
Propeller Secured?	<input type="checkbox"/>	Payload Secured?	<input type="checkbox"/>
Batteries Charged?	<input type="checkbox"/>	Aircraft	
Batteries Hot?	<input type="checkbox"/>	CG Verified?	<input type="checkbox"/>
Receiver Pack Charged?	<input type="checkbox"/>	Wing Securely Attached?	<input type="checkbox"/>
Receiver On?	<input type="checkbox"/>	Landing Gear Solid?	<input type="checkbox"/>
Connection Secured?	<input type="checkbox"/>	Top Lid Secured Shut?	<input type="checkbox"/>

Figure 7.4: Pre-Flight Checklist

Checks are performed immediately before the plane's takeoff, shown in Figure 7.5.

Final Checklist			
Propulsion		Signatures	
Receiver Connection?	<input type="checkbox"/>	Pilot	_____
Control Surfaces Responsive?	<input type="checkbox"/>	Faculty Advisor	_____
Telemetry Software On?	<input type="checkbox"/>	Project Manager	_____
Visual Inspection	<input type="checkbox"/>	Date	_____

Figure 7.5: Final Checks

Section 8

8.1 Component and Subsystem Performance

8.1.1 Propulsion

An Eagletree Elogger monitored battery performance during all flight tests. An example of these results is included as Figure 8.1, a mission 1 test. In Figure 8.1, the gold line is motor current, the blue is battery voltage, and the red is airspeed. As predicted, the batteries drained quickly during takeoff as that is the most intensive period of flight. The lower current sustained after takeoff allowed the batteries to continue for the duration of the mission. This flight ended with 75% voltage capacity, as tracked by the blue line in the figure. Please note that in Figure 8.1, the dip in current coupled with the increase in voltage about 25% into the data, lasting for 10-20 seconds, is due to a throttle back after initial climb-out. Voltage at low throttle is not well captured by the sensor as it is out of the effective range.

Mission 1 tests were successful for propulsion performance, except for landing, for which the propeller hub and blades were rendered unfit for flying. Some landings damaged propeller blades, because the motor was still spinning on landing. This was anticipated, and the Team plans to use a metal hub instead of the plastic one during competition. The Team will also program a motor brake to stop propeller motion for landing. After inspection, especially hard landings fractured the motor mount in addition to abrasions on the replaced propeller hub and blades. The motor mount was redesigned to be more durable for these instances.

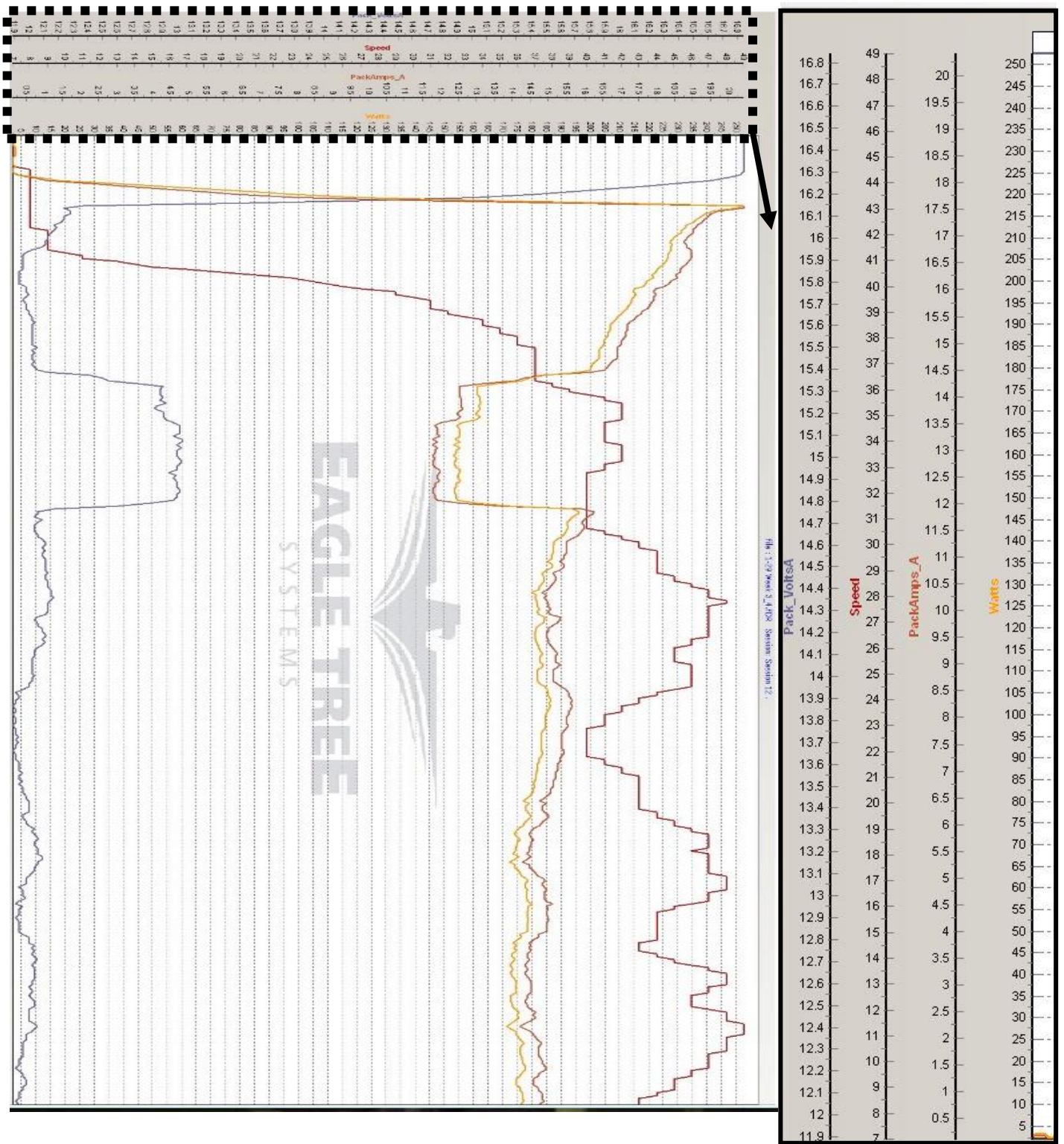


Figure 8.1: Mission 1 Propulsion Data

8.1.2 Structures

The Team tested both the fuselage and the wing to support the max payload. Wings were tested with the wingtip test described in Section 7. Broken payload bays were only observed to fail when the nose of the plane (motor mount) contacts the ground first during crashes, this is not a normal flight condition, and an acceptable failure. No wing or tail pieces have been tested to failure.

Prototypes have been drop tested inside of the tube, and both the plane and launch tube have passed the ground mission without damage.

8.1.3 Stability and Flight Test Results

Two prototype wing configurations have been tested so far. The first prototype was unstable in roll, this issue was addressed via modifications to aileron control authority and the second prototype was much more stable. The cruise speed of future prototypes needs to be raised to achieve 60mph loaded flights.

8.1.4 Prediction Comparisons and Improvements

All of the structures have performed as predicted, demonstrating sufficient strength for flight conditions. Once the next prototype is completed, all critical structures will be tested to failure to ensure that the Margin of Safety is not excessive. If so, the Team will lighten and weaken the structures.

8.2 Complete Aircraft Performance

The actual performance as measured from sensors onboard flight tests is compared to predicted performance in Tables 8.1 and 8.2.

	Turn Rate (deg/s)	Cruise Speed (mph)	1 Lap Time (s)	Battery Pack Endurance (min)
Actual	70	40	49	5.7
Predicted	67.8	49.38	40.1	6

Table 8.1: Mission 1 Results

	Turn Rate (deg/s)	Cruise Speed (mph)	1 Lap Time (s)	Battery Pack Endurance (min)
Actual	65	40	57	5.2
Predicted	35.73	47.17	55.34	6

Table 8.2: Mission 2 and 3 Results

8.2.1 Prediction Comparisons and Improvements

Tables 8.1 and 8.2 show that the plane outperformed predicted turn rate, this is likely due to the pilot being more aggressive than the simulation in applied g-loading during turns. Cruise speed was lower than predicted, this is due to drag or weather conditions that were not modeled. The lap times and pack endurance were also worse than predicted, and this was due to the slower cruise speed and un-modeled drag. In order to better achieve predicted performance, the Team will focus on minimizing sources of

parasitic drag, such as exposed electronics and control rods, as well as exploring increases in propulsion power.

8.3 Future Work

The Team intends to continue building prototypes, optimizing and iterating based on the analyses in this report. The Team intends to perform detailed structural testing on all retired components to optimize structural design. The Team also intends to implement a stabilization system to assist the pilot in maximizing mission performance. All prototypes will be flight tested in all missions. Once the design has been tuned to an optimal configuration, the competition aircraft will be constructed. This design will be test flown, tuned, and prepped for the competition in Tucson.

References

Reference 1:

Anderson, J. D., Fundamentals of aerodynamics, Boston: McGraw-Hill Higher Education, 2007.

Reference 2:

"Tail Design and Sizing," Tail Design and Sizing Available:
<http://adg.stanford.edu/aa241/stability/taildesign.html>.